

**Modeling Impact of Urbanization on Land Surface Temperature and
Assessment of Urban Heat Island Effect using Landsat: A Case Study of
Rawalpindi**



By

Tahira Saeed

(2020-NUST-MS-GIS-327747)


**A thesis submitted in partial fulfillment of the requirements for the degree
of Master of Science in Remote Sensing and GIS**

**Institute of Geographical Information Systems
School of Civil and Environmental Engineering
National University of Sciences and Technology
Islamabad, Pakistan**


September 2024

THESIS ACCEPTANCE CERTIFICATE


Certified that final copy of MS/MPhil thesis written by **Tahira Saeed (Registration No. MSRSGIS 00000327747), of Session 2020 (Institute of Geographical Information systems)** has been vetted by undersigned, found complete in all respects as per NUST Statutes/Regulation, is free of plagiarism, errors, and mistakes and is accepted as partial fulfillment for award of MS/MPhil degree. It is further certified that necessary amendments as pointed out by GEC members of the scholar have also been incorporated in the said thesis.

Signature: 
Name of Supervisor: Dr Javed Iqbal
Date: 30-8-24

Dr. Javed Iqbal
Professor & IGIS SCEE (NUST)
H-12 Islamabad

Signature (HOD): 
Date: 18-9-24

Dr. Muhammad Ali Tahir
HoD & Assoc. Prof. SCEE (IGIS)
NUST, H-12, Islamabad.

Signature (Principal & Dean SCEE): 
Date: 19 SEP 2024

PROF DR MUHAMMAD IRFAN
Principal & Dean
SCEE, NUST

ACADEMIC THESIS: DECLARATION OF AUTHORSHIP

I, **Tahira Saeed**, declare that this thesis and the work presented in it are my own and have been generated by me as the result of my own original research.

“Modeling Impact of Urbanization on Land Surface Temperature and Assessment of Urban Heat Island Effect using Landsat: A Case Study of Rawalpindi”

I confirm that:

1. This thesis is composed of my original work, and contains no material previously published or written by another person except where due reference has been made in the text.
2. Wherever any part of this thesis has previously been submitted for a degree or any other qualification at this or any other institution, it has been clearly stated.
3. I have acknowledged all main sources of help.
4. Where the thesis is based on work done by myself jointly with others, I have made clear exactly what was done by others and what I have contributed myself.
5. None of this work has been published before submission.
6. This work is not plagiarized under the HEC plagiarism policy.

Signed:



Date: 23/09/2024

DEDICATION

To

My Parents, family and friends

Thanks to their unwavering support, care and motivation since the beginning of my studies and throughout my research work.

ACKNOWLEDGEMENTS

All praises, obedience, and submission to ALMIGHTY ALLAH, the propitious, the benevolent and sovereign whose blessings and glory flourish my thoughts and thrive my ambitions. I have the only pearls of my eyes to admire the blessings of the compassionate and the omnipotent because the words are bound, knowledge is limited, and time is short to express His dignity. My special praise for Holy Prophet Muhammad (PBUH) who is forever a torch of knowledge for humanity.

I wish to express special thanks to my supervisor Dr. Javed Iqbal, and Lect. Junaid Aziz Khan, National University of Science and Technology (NUST) for their wonderful patronage and supportive attitude in helping me throughout the technicalities of my research.

I would also like to express my gratitude to Dr. Ejaz Hussain (IGIS) and Dr. Erum Aamir (IESE) who helped me a lot during my research work and thesis completion and supported me morally.

Also, a heartfelt thanks to all my friends who have been with me through thick and thin providing support and encouragement. Their friendship and assistance have been instrumental in completing this project, and I am deeply grateful for their contributions.

TAHIRA SAEED

TABLE OF CONTENTS

THESIS ACCEPTANCE CERTIFICATE.....	ii
ACADEMIC THESIS: DECLARATION OF AUTHORSHIP.....	iii
DEDICATION.....	iv
ACKNOWLEDGEMENTS	v
LIST OF FIGURES	viii
LIST OF TABLES.....	ix
ABBREVIATIONS	x
ABSTRACT.....	xi
CHAPTER 1: INTRODUCTION.....	1
1.1. Background Information.....	1
1.2. Increasing Urbanization and LULC change	2
1.3. Rising Land Surface Temperature	4
1.4. Urban Heat Island Formation	5
1.5. Utilizing Remote Sensing and GIS for UHI Analysis.....	6
1.6. Relevance to National Needs.....	7
1.7. Research Objectives.....	8
CHAPTER 2: LITERATURE REVIEW.....	10
CHAPTER 3: MATERIALS AND METHODS.....	16
3.1. Study Area	16
3.2. Methodology Flowchart.....	18
3.3. Datasets used	20
3.4. Software Used.....	21
3.5. Land Use Land Cover Mapping	22
3.6. Accuracy Assessment	24
3.7. Retrieving Land Surface Temperature	25
3.7.1. Converting Digital Number (DN) values to Spectral Radiance	25
3.7.2. Conversion to Top of Atmosphere (TOA) Radiance	26
3.7.3. Conversion of Spectral Radiance L_{λ} to Brightness Temperature T_B	26
3.7.4. Calculating Spectral Emissivity.....	27
3.7.5. Calculating Land Surface Temperature.....	27
3.8. Derivation of Spectral Indices.....	28
3.9. Correlating Indices with LST	29

3.10. UHI Analysis through Calculating UTFVI.....	29
3.11. Survey Conduction.....	30
CHAPTER 4: RESULTS AND DISCUSSION	32
4.1. Land Use Land Cover.....	32
4.1.1 Land Use Land Cover Change Detection.....	40
4.2. Land Surface Temperature Retrieval.....	41
4.3. Correlation of Spectral Indices with LST	42
4.4. Urban Thermal Field Variance Index	50
4.5. Results from Survey Conduction.....	53
4.6. Relevance with Sustainable Development Goals	56
CHAPTER 5: CONCLUSION AND RECOMMENDATIONS.....	57
REFERENCES.....	59

LIST OF FIGURES

Figure 1. The study area map.....	17
Figure 2. The methodology flowchart.....	19
Figure 3. Random forest classifier	23
Figure 4. Code script for LST retrieval.....	25
Figure 5. Training points for supervised classification	33
Figure 6. The study area land use/land cover classification for the year 2003	34
Figure 7. The study area land use/land cover classification for the year 2008	34
Figure 8. The study area land use/land cover classification for the year 2013	35
Figure 9. The study area land use/land cover classification for the year 2018	35
Figure 10. The study area land use/land cover classification for the year 2023	36
Figure 11. The study area built-up increase from 2003 to 2023	41
Figure 12. The study area land surface temperature of 2003	43
Figure 13. The study area land surface temperature of 2008	44
Figure 14. The study area land surface temperature of 2013	45
Figure 15. The study area land surface temperature of 2018	46
Figure 16. The study area land surface temperature of 2023	47
Figure 17. The study area UTFVI maps for years 2003, 2008, 2013, 2018, and 2023	52
Figure 18. Survey question 1 response	53
Figure 19. Survey question 2 response	54
Figure 20. Survey question 3 response	54
Figure 21. Survey question 4 response	55
Figure 22. Survey question 5 response	55

LIST OF TABLES

Table 1. Data sets Used.....	20
Table 2. The UTFVI reference values.....	30
Table 3. Overall accuracy assessment of classified image (2003).	37
Table 4. Overall accuracy assessment of classified image (2008).	37
Table 5. Overall accuracy assessment of classified image (2013).	38
Table 6. Overall accuracy assessment of classified image (2018).	38
Table 7. Overall accuracy assessment of classified image (2023).	39
Table 8. LULC change (Km ²).....	40
Table 9. Temporal change in LST and built-up.....	48
Table 10. Correlation of NDVI with LST	48
Table 11. Correlation of NDBI with LST.....	49

ABBREVIATIONS

ETM+	Enhanced Thematic Mapper Plus
EVI	Enhanced Vegetation Index
GEE	Google Earth Engine
GIS	Geographic Information System
GVF	Green Vegetation Fraction
IPCC	Intergovernmental Panel on Climate Change
LULC	Land Use Land Cover
LST	Land Surface Temperature
NDVI	Normalized Difference Vegetation Index
NDBI	Normalized Difference Built up Index
NIR	Near Infra Red
PMD	Pakistan Meteorological Department
PRECIS	Providing Regional Climates for Impact Studies
RS	Remote Sensing
SWIR	Short Wave Infra Red
SUHI	Surface Urban Heat Island
UNDP	United Nations Development Fund
UTFVI	Urban Thermal Field Variance Index

ABSTRACT

Unplanned urbanization is an escalating issue in Pakistan, particularly in cities like Karachi, Lahore, Faisalabad, and Rawalpindi. With the highest urbanization rate in South Asia, Pakistan is projected to have 50% of its population in cities. This study focuses on the impact of increasing urbanization on Land Surface Temperature (LST) and examines the effects of surface urban heat island formation in Rawalpindi. Land use changes were analyzed through supervised image classification of satellite imagery, and LST was calculated using machine learning and cloud-based computing in Google Earth Engine. The results indicate that the built-up area in Rawalpindi expanded from 74.5 km² in 2003 to 227.7 km² in 2023, reflecting a 206% increase over 20 years. The LST trends show a significant rise, with the mean LST increasing from 34°C in 2003 to 39°C in 2023. The correlation analysis between LST and spectral indices—NDVI (Normalized Difference Vegetation Index) and NDBI (Normalized Difference Built-up Index)—revealed a positive relationship between LST and NDBI, and a negative relationship between LST and NDVI. This suggests that LST rises with increasing built-up areas and barren land while it decreases in densely vegetated regions. Additionally, the Urban Thermal Field Variance Index (UTFVI) for Rawalpindi showed that most built-up areas fall under the severe UTFVI effect category. Survey results further indicate that residents perceive the severity of summer months to have worsened over time, adversely affecting population health and resource availability. Heat-related illnesses, including heat exhaustion, heat stroke, gastric issues, and dehydration, have become more common with rising LST levels. This study provides critical insights into land use and land cover (LULC) changes and UTFVI, offering valuable information for urban planners to understand the urban climate better and implement effective mitigation strategies.

INTRODUCTION

1.1. Background Information

Climate change is a global phenomenon that largely impacts urban life and is also impacted by the increasing number of urban areas globally. Cities are considered as a major contributor to climate change as urban activities such as transportation, industrialization and land use changes are major sources of greenhouse gas emissions. According to the IPCC (2022) report, urban areas are estimated to be responsible for about 70% of the global greenhouse gas emissions. Today, more than half of the world's population lives in cities, and it is projected that by 2050, about 68% of the global population will be living in urban areas. Urbanization is one of the major driving forces behind land use land cover change and a great deal of urbanization is depicted as urban sprawl, that is an extensive form of land use change with environmentally detrimental effects (Nuissl & Siedentop, 2021). Urbanization is thus significantly linked to alterations in various landforms such as bare land, vegetation, agricultural land and built-up areas, consequently impacting the land surface temperature and leading to the formation of urban heat islands. The rapid expansion of urban areas and changes in land use patterns can be linked to population growth and economic activities that can further exacerbate the issue through unplanned and unmanaged urban development (Bimenyimana et al., 2022). Urbanization can also create significant changes in the atmospheric properties that can further alter the local weather and climate. The local effect is primarily associated with the urban characteristics such as scarceness of vegetative cover, abundance of paved surfaces, increased long wave radiation due to higher pollution at the top of an urban area, and excessive use of energy required for the effective functioning of cities. These

urban characteristics significantly impact land, water, surface temperature, environment and ecology. Urbanization largely affects the climatic conditions by decreasing precipitation, evaporation rate and hydrology area and rise in the land surface temperature (Faisal et al., 2021). Land surface temperature in densely populated cities tends to be elevated as compared to the surrounding rural or sub-urban areas. Temperatures can also vary within the cities in relation to the spatial distribution of soil, water, vegetation and impervious surfaces. Moreover, the natural cooling effect from evapotranspiration and shading is minimized due to reduced vegetation in urban areas. Air conditioning units, buildings, vehicles and industrial facilities also further add on to the emitted heat into the urban environment. Surface urban heat islands represent the radiative temperature difference between the natural and impervious surfaces. The formation of urban heat islands can increase the risk of heat-related illnesses as increased urban heat island intensity can contribute to heat cramps, exhaustion, dehydration, heat stroke, respiratory difficulties and headaches. It can also impact other factors such as increased electricity demand, increased emission of greenhouse gases and air pollutants, power outages, formation of ground-level ozone and degraded water quality mainly due to thermal pollution (Singh et al., 2020).

1.2. Increasing Urbanization and LULC Change

Globally, more than 50% of the population is living in cities and it is projected that by 2050, more than 70% of the global population would be living in cities. Pakistan is categorized among the fastest urbanizing countries particularly in South Asia and is urbanizing at an annual rate of 3% (Jabeen et al., 2017). Increase in population and migrations drive a majority of the country's urbanization owing to multiple factors such as escaping war or conflict, natural disasters, insecurity and search of better services and livelihood. The population in the country has increased from 50 million in the 1960s to more than 230 million in 2022. Urbanization can be promising in terms of

boosting the economy, however, unplanned and mismanaged urbanization in Pakistan has given rise to several problems and has resulted in the formation of urban slums. Some major issues arising from unmanaged urbanization are transportation, health, housing, water and sanitation, land management and land surface temperature in cities. Pakistan has a largely arid climate with varying humidity, hot summers, and cold winters. There is a major temperature difference between urban and rural areas of the country, with urban areas facing high heat indexes. The significant urbanized cities in Pakistan are Karachi, Lahore, Faisalabad, Rawalpindi, Islamabad, Peshawar, Sargodha and Mardan.

Urbanization is a major contributing factor behind the current climate crisis in Pakistan, resulting in high temperatures and heat waves, which create significant changes in land surface and atmospheric properties that can alter the local weather. The local heating effect is also associated with scarce vegetation, paved surfaces, decreased albedo and increased longwave radiation due to high pollution in urban areas (Moazzam et al., 2022). This also drives significant changes in land use land cover (LULC) of a region due to the construction of new buildings and road infrastructure and an increase in impervious surfaces. In the last three decades, green spaces have significantly decreased in Rawalpindi due to an increase in urban area by approximately 37% and a population that has increased significantly from less than 1.5 million in 2000 to more than 2.4 million in 2024 according to global metrics (ul Haq et al., 2021). The alteration of land surfaces with concrete and asphalt materials reduces the available surface moisture and contributes to anthropogenic heat generated by buildings, vehicles or machinery people use (Sajjad et al., 2020a). Changes to landscapes can increase stress on biogeochemical processes, hydrological cycles and environmental sustainability of natural resources. Multiple studies have utilized time series

satellite images to quantify land use land cover change and to make LULC classes through supervised or unsupervised classification techniques (Nath et al., 2021).

1.3. Rising Land Surface Temperature

Globally, a 1.5 °C difference is found between Land Surface Temperature LST and Sea Surface Temperature SST as land surface temperatures continue to exceed sea surface temperatures, mainly due to higher heat capacity of oceans as compared to nearby land. Urban expansion and growth are significantly related to increased land surface temperatures due to building materials (Sandoval et al., 2023). Urban expansion is characterized by replacement of topsoil and foliage by concrete surfaces of roads, bridges, and residential, commercial or industrial buildings. This conversion of natural surfaces to impervious landforms leads to changes in the biophysical climate leading to an increase in the LST (Sajjad et al., 2020). Increased number of built-up areas can increase the land surface temperature as surface temperature is higher in urban areas as compared to the vegetated and water covered areas. Urban areas have higher heat absorption and retaining capacity than the surrounding rural areas. The materials used in construction in urban areas such as asphalt and concrete have a high thermal mass due to which they absorb large amounts of heat during the daytime and slowly release heat at night due to their higher retention capacities, thus preventing night time cooling effect. The composition and configuration of land use land cover strongly relate to the landscape pattern and thermal characteristics associated with LST. In the urban areas, there are various key determinants of variation in land surface temperature such as soil functions, vegetation abundance and impervious surfaces (Jain et al., 2020). In urban areas, natural landscapes are limited, and urban infrastructures are highly concentrated due to which, the temperature in urban areas is significantly higher than the surroundings. Developing countries such as Pakistan are facing significant environmental risks and climatic challenges due to the inability

to tackle rapid urbanization and population growth (Ameen & Mourshed, 2017). Particularly the twin cities, Rawalpindi and Islamabad have faced rapid urbanization due to the movement of people from rural areas and other underdeveloped cities. Such rapid urban expansion caused by the massive population changes have resulted in substantial changes in land use and the local ecology of the cities.

1.4. Urban Heat Island Formation

Urban Heat Islands UHI can be defined as those urbanized areas that experience higher temperatures in contrast with the non-urban outlying areas. Urbanization is also an important causative factor of climate change due to increased greenhouse gas emissions owing to vehicle use and energy consumption. These increased greenhouse gases can act as a partial blanket in the atmosphere that can store solar energy radiation, further leading to an increase in the surface temperature. These changes in the land surface temperature due to the impervious surfaces and heat retaining capacity of land and atmosphere give rise to the urban heat island formation (Yang et al., 2016). Urban heat island formation depends on factors such as population density, nature of urban landscape, meteorological conditions and anthropogenic activities. Heat islands are mainly formed when vegetation is replaced by buildings, asphalt and concrete for roads and other urban structures that are necessary to maintain growing populations. The urban heat island effect is further worsened by improper urban planning and air pollution leading to high ground ozone concentrations that prevent heat from rising into the atmosphere (Anbazu & Antwi, 2023). Due to the intense urban heat island effect, urban hotspots can develop where residents have to experience high heat stress, which consequently results in excessive energy use. Moreover, urban heat islands can damage various sectors such as commerce, health, industries, infrastructure, agriculture and education. This heat island effect becomes more noticeable and adverse after sunset as heat stored

throughout the day in land surfaces is released slowly over the night. Urban heat islands are closely linked to the rise of heat related illnesses such as heat exhaustion, heat stroke and numerous vector borne diseases in tropical cities that can even lead to fatalities (Abir et al., 2021). Pakistan is also experiencing this urban heat island effect in majority of its metropolitan cities evident from the high heat indexes that have resulted in a climate crisis in the country. According to the Global Climate Risk Index, Pakistan is the fifth most susceptible country to climate change, with heat-related risks accounting for the majority of this vulnerability (Asad et al., 2023). The extreme weather in Pakistan begins from May and extends up to September where the major effect of urban heat island is associated with heatwaves. Rapid urbanization and global warming impacts have inflicted massive urban heat island effect in major cities such as Karachi and Lahore where exposure to heat is highly associated with -related illnesses such as heat stroke and heat exhaustion, particularly for elderly people and those working outdoors. Increased heat can also exacerbate various underlying conditions such as diabetes, asthma and cardiovascular diseases.

1.5. Utilizing Remote Sensing and GIS for UHI Analysis

Remote Sensing (RS) and Geographic Information System (GIS) are computer-based technologies for collecting, managing, manipulating, analyzing, modelling and presenting geographically referenced data. With the advancements in RS and GIS technologies, and incorporation of machine learning, spatial modelling approaches and cloud-based platforms such as Google Earth Engine (GEE), the processes related to analyzing and mapping urbanization have become highly efficient. Various RS and GIS approaches can extract data including land use, land cover, land surface temperature, population density, and energy consumption, which can then be utilized to study existing and future urbanization patterns. Remote sensing techniques can provide powerful tools for analyzing spatio-temporal and spectral phenomena of changes in the land use land cover at

various local, national and international levels. Satellite imagery can be used to capture high spatio-temporal resolution data for land use and land cover changes over a period of time. This data can be further classified into multiple categories based upon the range of analysis. Satellite imagery is also useful in detecting the LST by utilizing satellite thermal infrared data with high spatial resolution and accuracy. LST is further used to evaluate the environment's thermal wellbeing through analyzing the urban heat island effect through changes in the rural and urban temperatures. GIS techniques can then be used to create detailed maps for a thorough visual analysis and further processing and interpretation of the data (Murayama et al., 2021). Plenty of global research has been conducted on the impacts of urban heat islands on various geographic distributions and resultant urban vulnerability and risks have been analyzed using remote sensing techniques and quantitative measures. One such quantitative technique is the Urban Thermal Field Variance Index (UTFVI), a widely used indicator, employed to quantify the urban heat island by exploring the spatio-temporal heterogeneities in temperature. A high UTFVI can cause multiple adverse impacts such as declining air quality, changes in local wind patterns and humidity, rising mortality rates and worsening weather patterns (Kafy et al., 2020).

1.6. Relevance to National Needs

Unplanned and unmanaged urbanization and urban sprawl is a rising problem in various big cities of Pakistan, particularly including Karachi, Lahore, Rawalpindi, Faisalabad, Peshawar and others. This unmanaged urbanization is leading to the problems of economic burden in megacities, urban slums formation, population influx and environmental degradation in terms of rising land surface temperature. In Pakistan, the seasonal temperature rises are found to be higher than the global average due to the country's geographical location. The country has a huge housing deficit, according to a UNDP report, and the numbers are considered to reach nearly 10 million units,

contributing to housing shortages and the growth of slums without any systematic urban planning. This impacts natural resources and exerts pressure on nearby rural areas, thus contributing to major changes in land use and land cover. Urban sprawl has led to an increase in the built-up area, leading to land degradation, loss of vegetation and fertile agricultural lands, ecosystem degradation, and increased flood susceptibility. Moreover, the rising land surface temperature is contributing to the formation of urban heat islands, resulting in heat waves, climate change, higher pollution levels and increased energy consumption. High urban temperatures have also contributed to human health degradation in Pakistan's major cities. As Pakistan mostly has an arid to semi-arid climate, it is highly threatened by the global climate change as it is predicted that by the end of this century, temperatures will rise about 5-6°C. This rise in temperature is further accompanied by the growing LST due to increasing urbanization. This has given rise to increasing problems of insufficient medical facilities, formation of urban slums, heat related illnesses, and environmental degradation. The study aims to analyze the impact of rising temperatures in the form of UHI formation and its adverse impacts on the population, environment and resources along with suggesting appropriate remediation strategies to manage urbanization.

1.7. Research Objectives

The objectives for this study are,

- To generate spatiotemporal (2003 to 2023) Land Use and Land Cover (LULC) and Land Surface Temperature (LST) change maps.
- To correlate the relevant factors with LST and quantify the urban heat island effect through the Urban Thermal Field Variance Index UTFVI.

- To analyze the multivariate relationship between urban heat island effect and socio-economic factors such as population health, energy consumption, and availability of essential living resources through survey conduction.

LITERATURE REVIEW

The increase in global population and rapid migration to urban areas has led to extensive urbanization as 50% of the global population is now an urban resident. Urbanization leads to the development of cities that can serve as a source for economic growth, pertaining to effective management and systematic urban planning and development. However, urbanization affects the natural habitats and increases resource consumption, contributing to enhanced greenhouse gas emissions. This exerts pressure on the natural environment, leading to global warming and climate change on the local, national and international levels. Urbanization is the major causative factor behind changes in the land use land cover, mainly evident in terms of reduction in green spaces and rise of concrete and impervious surfaces, further contributing to an increase in the LST and resultant detrimental impacts on population health and environment (Slimani & Raham, 2023).

The major cities of Pakistan have expanded tremendously owing to the population growth, leading to an increase in the urban population density. Dense urbanization is a major causative factor behind rapid rise in the urban heat island effect. Several studies have been carried out on the impacts of urbanization and land use change on the land surface temperature and the resultant formation of urban heat islands. (Sajjad et al., 2020b) conducted a study on the impact of urbanization on local temperature trends of twin cities, Rawalpindi and Islamabad. Landsat images of four years, 1980, 1992, 2000 and 2013 were used and classified through supervised image classification with probability surface method and maximum likelihood rule to conduct this study. Moreover, changes in temperature trends were evaluated through time series data analysis using regression for the period 1983 to 2013. The study's results indicated an increase in built-up areas

in both Rawalpindi and Islamabad along with increasing temperature trends particularly during the spring season.

Ahmad et al., (2022) conducted a study on the LST dynamics and the impact on land cover in the district of Peshawar, Khyber Pakhtunkhwa. This study utilized four Landsat images from 1990 to 2019 with a 10-year gap and utilized them for land cover mapping and retrieval of LST. The supervised classification method was used to generate LULC, and the rainfall data and air temperature for the selected years were obtained from Pakistan Meteorological Department PMD for further analysis and validation. The results of land cover classification and analysis showed that the built-up area had increased from 14.2% to 20.22% during 1990 to 2019 while the results of the LST also show that the UHI effect that was previously concentrated mostly in the barren land has expanded mainly in the areas with impervious surfaces and roads. A drastic increase in the LST values with highly expanded UHIs was observed in the central region of the study area.

Farid et al., (2022) conducted a study monitoring the impact of rapid urbanization on the land surface temperature and assessment of surface urban heat island in Lahore using Landsat. Land use changes were observed through data acquisition from Landsat TM and OLI from 1990 to 2020 using the supervised classification method. The study concluded that urbanization impacted the city's overall LST with increased built-up area. Moreover, the difference between rural and urban buffer revealed that Surface Urban Heat Island (SUHI) was also increasing over the years. The study also reveals that LST is inversely related to normalized difference vegetation index (NDVI) as the decrease in vegetated area increases the land surface temperature.

Another study regarding the impact of land use land cover change on the distribution of land surface temperature in Ho chi min city, Vietnam was conducted by Ha et al., (2021). Urbanization plays a key role in the urban climate change and development of urban heat islands. The impacts

of land cover change on the land surface temperature were assessed by applying GIS and remote sensing data. Multitemporal Landsat data was acquired from the year 1998 to 2020. Landcover maps were generated through classification using the object-oriented method. Land surface temperature was calculated by the conversion of pixel values of the thermal band of Landsat to spectral radiance. The overall study indicated an increase in the urban area with resultant high LST ranging from 20.2°C to 31.2°C in 1998 to 22.1°C to 42.3°C in 2020 for Ho Chi Min city.

A study regarding the monitoring and analysis of urban heat island of Lahore particularly during the winter season was conducted by Basit et al., (2019) in which the impact of temperature variations and urbanization was studied. Digital weather stations were installed in the winter season of 2015 at two sites, one urban and the other rural. Moreover, meteorological data were collected on a diurnal basis for four days with an interval of 30 minutes to check the intensity of temperature difference at both sites. The study results showed notable differences between the temperature of urban and rural sites. Moreover, there is strong evidence in the study suggesting that rapid urbanization, more energy consumption, lack of vegetation and more urban population contributed to the high temperature and formation of urban heat islands.

Waseem & Athar, (2022) studied the variability of land surface temperature and population growth in the Rawalpindi district from 1993 to 2018. Variability of LST due to the variation in vegetative cover in the city was assessed through satellite data from Landsat thematic mapper in two tehsils, Rawalpindi and Taxila. Retrieval of LST from Landsat thermal band was performed through the semi-automatic classification plugin in QGIS software. A regional climate model PRECIS (Providing Regional Climates for Impact Studies) was used to correct the bias of satellite-based LST. The LST variability was analyzed using probability density functions for both tehsils. The inter-relationship of LST and population magnitude was quantified through various statistical

operations such as calculating the mean, skewness, kurtosis, standard deviation, displaying scatter plots and performing ordinary least squares-based regression analysis. The study's results suggested a strong correlation between the census data and LST. Moreover, a negative correlation between LST and Green Vegetation Fraction (GVF) indicates a decrease in vegetation cover, which contributes to an increase in LST.

Waleed & Sajjad, (2022) conducted a study to analyze spatio-temporal land use land cover patterns and provide insights regarding LST rise in Punjab, Pakistan, using data from past three decades of 1990 to 2020. The study leveraged various spatial modeling techniques and cloud-based computing to provide spatio-temporal insights regarding the LST variations in relation to changes in land use land cover. The study utilized the random forest algorithm, cloud computational capabilities of Google Earth Engine GEE and tier-1 data of Landsat missions, mainly Landsat 5 and Landsat 8 along with the relevant spectral indices such as Enhanced Vegetation Index EVI, Normalized Difference Vegetation Index NDVI, Normalized Difference Water Index NDWI, Soil Adjusted Vegetation Index SAVI etc. to evaluate the association between LULC and several LST types. Heat charts for LST were also created for Punjab's top twenty cities based on population to illustrate LST summary figures for various time periods, 1990, 2000, 2010, and 2020, respectively. The produced maps in the study serve as a useful insight for city planners to formulate appropriate cooling measures to reduce the UHI and strategies for promoting the stability of land resources in the study area.

Arshad et al., (2020) assessed the vulnerability of urban growth in Karachi and modeled green areas to enhance heat wave risk resilience. The GIS and RS techniques have been used to identify the status of urban green spaces in the city and to estimate the suitability of forest scenario projection models. The study utilized meteorology datasets to quantify the frequency of heat waves

in the study area and the downscaling of temperature rise under the future scenarios. The results revealed that the enhanced occurrences of heat waves had a strong connection with the extreme weather events and climatic changes that were triggered by several factors such as industrialization, emissions of carbon dioxide, urbanization, degradation of mangrove forests, deforestation and land use changes. This study aims to promote smart sustainable city planning among planners and citizens by offering an early evaluation and precise policy implications in meteorological predictions for the establishment of early heat wave warning systems.

Jain et al., (2020) conducted a study on the intensity of urban heat island in Nagpur city in Maharashtra and also analyzed the mitigation strategies that can be adopted in fast-growing urban areas. The study employed time series Landsat data of Thematic Mapper TM and Enhanced Thematic Mapper Plus ETM+ to analyze the LST and quantify the UHI effect for the study area for the years 2000, 2005, 2010 and 2015. Various spectral indices such as NDVI, NDBaI, and NDBI were used to analyze the biophysical characteristics of the study area. In order to investigate the sensitivity of temperature and greenness throughout the city region, seasonal LST and the biophysical makeup of the city have been examined. In the summer and autumn/spring seasons, there was a positive correlation between the city's per capita electricity use and the surface LST. A relative brightness temperature method was utilized to investigate the type of UHI present throughout the city. It was evident from the results that the temperature was particularly high in the city core, and certain peripheral regions of the city also showed a higher temperature, mainly due to the destruction of vegetation and developments taking place in the outer parts of the city.

Sameh et al., (2022) conducted a study investigating the impact of LULC class changes on LST through automated mapping of urban heat island to identify the distribution of urban hotspots in Mansoura city, Egypt. Using Landsat imagery from 1990 to 2021. Artificial neural network

approaches, cellular automata and machine learning algorithms were used to predict the future changes for LST and LULC for the year 2031. This study also utilized UTFVI to quantify the influence of UHI in the study region. The results revealed that NDBI had a positive correlation with LST while NDBI had a negative correlation with LST. The forecast results show that built up area will grow by 20% by 2031, and vegetation will decrease by 18% with enhanced UTFVI influence.

Numerous studies have analyzed the LULC changes through using various classification techniques in GIS mapping and cloud-based computing platforms. UTFVI has widely been used as an index to quantify the UHI effect as it provides a means to evaluate the intensity and spatial distribution of heat islands within urban areas. UTFVI also allows users to identify the specific hotspots within urban areas allowing localized temperature analysis for targeted mitigation strategies (Kusumawardani & Hidayati, 2022). This study also utilizes the LULC and LST data obtained from satellite imagery to quantify the UTFVI effect in Rawalpindi, along with analyzing the impact of rising temperatures and urban heat island formation on the socio-economic factors for the residents of Rawalpindi such as population health, availability of resources and energy consumption through conducting a survey.

MATERIALS AND METHODS**3.1. Study Area**

The Rawalpindi district is divided into 7 tehsils: Gujar Khan, Kahuta, Kotli Sattian, Kallar Syedan, Taxilla, Murree and Rawalpindi. The study area is Rawalpindi Tehsil, an administrative subdivision of district Rawalpindi, situated in the western part of Punjab province. Rawalpindi is the most populous tehsil of the district with a population of 3.26 million according to the 2017 census that has been rising tremendously as compared to the previous figure of 1.9 million according to the 1998 census. Geographically, Rawalpindi extends from 33.56 °N to 73.01 °E and is about 508 meters above sea level. The city's population is predominantly urban, with the city of Rawalpindi being a major urban center, with 64.4% of the population living in urban areas and 35.6% living in rural areas. Rawalpindi tehsil has a humid subtropical climate that is characterized by mild winters, hot summers and a monsoon season. In summer, temperatures often exceed 30 °C and can cross 40°C on hotter days. June is typically considered to be the hottest month in the area. Like many other expanding cities, Rawalpindi has faced challenges with urban sprawl. Urban boundaries have expanded into previously undeveloped or agricultural landforms due to rapid population growth and rural-to-urban migration. This expansion has resulted in increased pressure on the provision of public services, housing and transportation. Increasing urbanization in Rawalpindi has led to numerous environmental challenges such as depletion of green spaces, waste management issues, air and water pollution and rising urban heat island intensity in the main city region. Figure 1 shows the study area map illustrating the map of Pakistan, Punjab province and the study region, Rawalpindi Tehsil.

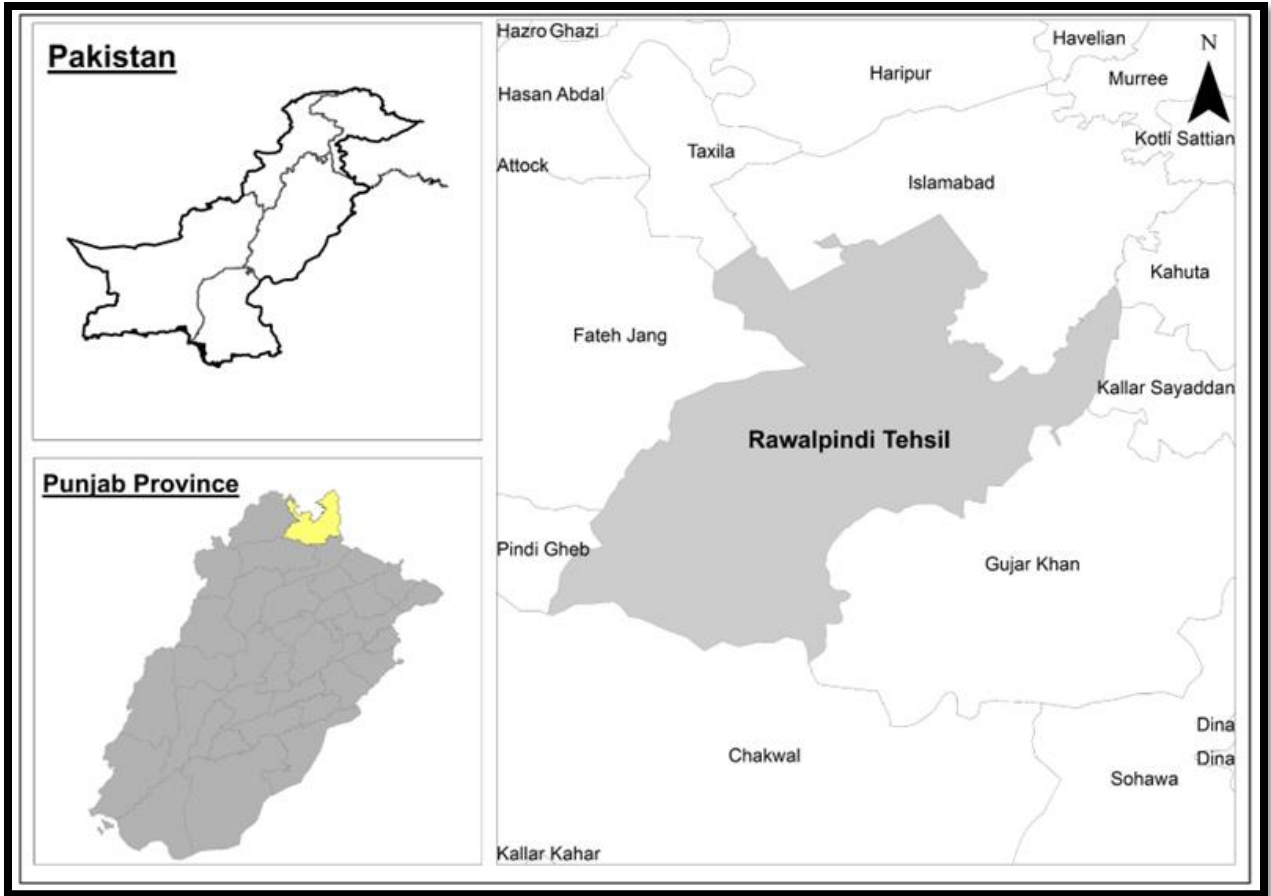


Figure 1. The study area map.

3.2. Methodology Flowchart

The three objectives of the study are met through following certain steps. Satellite images of the years 2003, 2008, 2013, 2018 and 2023 were obtained from the Earth Engine Data Catalog and land use land cover was classified using the Random Forest classifier into four classes: water bodies, built up, vegetation and bare land. The classification was performed by taking more than 300 training points for each class in the imageries to obtain accurate results. Detailed accuracy assessments were performed in ArcMap through comparing the classified images with the ground truth data from Google Earth Pro. Spectral indices for vegetation and built up including NDVI and NDBI were also obtained from the satellite images using respective bands such as NIR and red bands for NDVI and SWIR and NIR bands for NDBI. Time series LST maps were obtained from Google Earth Engine through calculating various factors such as spectral radiance, proportion of vegetation, emissivity and brightness temperature. LST maps were then correlated with the indices and LST data was also utilized to map the UTFVI for study region in the respective years. A survey was also conducted to analyze the impacts of rising temperature and urban heat island effect in Rawalpindi and their adverse impacts on population health and other socio-economic factors. Figure 2 shows the individual steps followed to achieve the three objectives of the study.

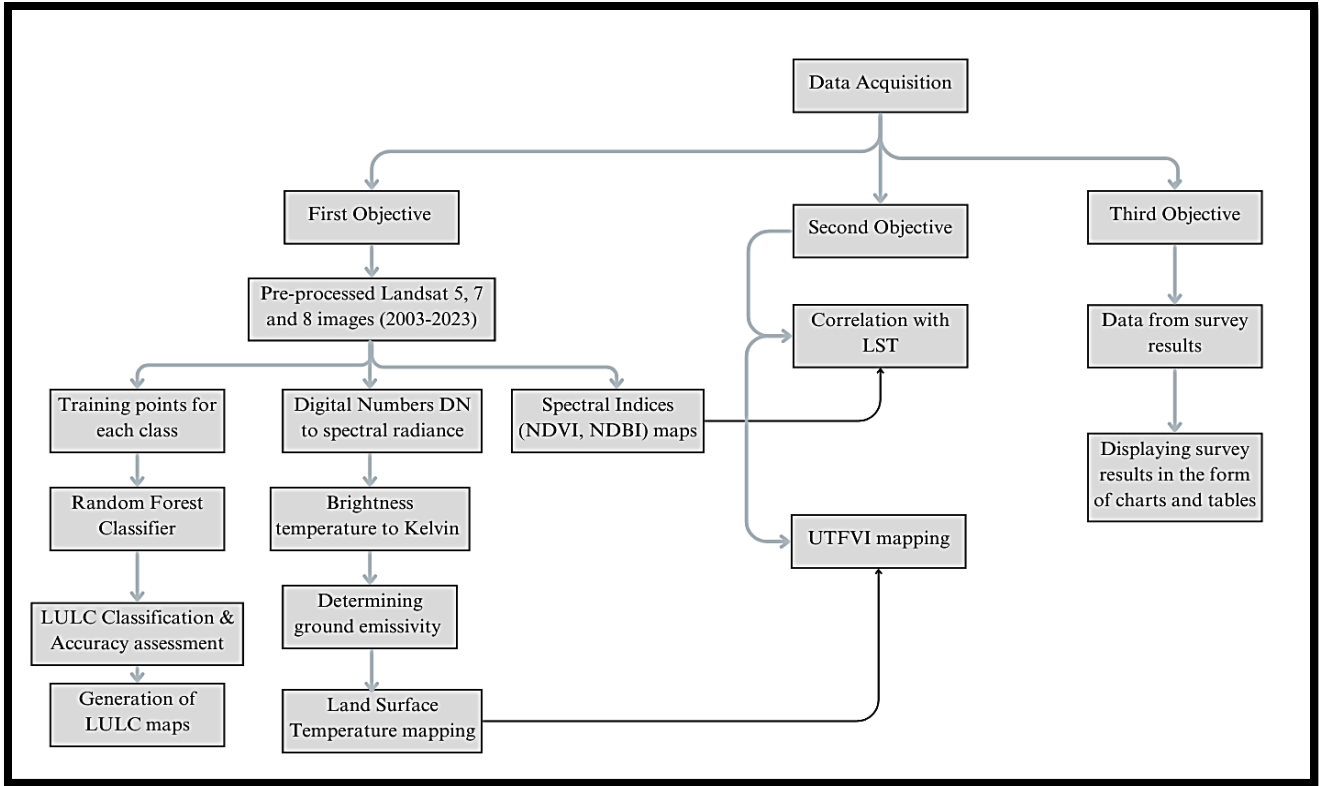


Figure 2. The methodology flowchart.

3.3. Datasets used

Landsat Collection 2 satellite imagery with 30-meter resolution was obtained from Earth Engine Data Catalog. Collection 2 is recognized as the Landsat archive's second major reprocessing effort, containing significant product improvements as well as advances in data processing and algorithm design. Collection 2 includes Landsat level 1 data for all sensors since 1972, as well as level 2 surface temperature and surface reflectance products for data obtained since 1982 (U.S. Geological Survey, 2021). Collection 2 products have more geometric accuracy, and improved processing and radiometric calibration as opposed to the previous products. This study utilized tier 1, collection 2, level 2 data of Landsat 8 OLI/TIRS, Landsat 7 ETM+ and Landsat 5 TM for the years 2003 to 2023, each image taken with a 5-year gap. Table 1 shows the datasets used for the study.

Table 1. Data sets Used

Type of dataset used	Year	Resolution	Source
Landsat 7	2003	30m	Earth Engine Data Catalog
Landsat 5 TM	2008	30m	Earth Engine Data Catalog
Landsat 8 OLI/TIRS	2013	30m	Earth Engine Data Catalog
Landsat 8 OLI/TIRS	2018	30m	Earth Engine Data Catalog
Landsat 8 OLI/TIRS	2023	30m	Earth Engine Data Catalog
Results from survey	-	-	Online survey conduction

3.4. Software Used

The GIS software used for this study was ArcMap 10.8, a mapping application developed by ESRI as part of its suite of geospatial processing programs. The software was used primarily for map creation and visualization, editing and managing spatial data, and performing various analyses and calculations to understand spatial patterns and relationships.

The study mainly utilized Google Earth Engine GEE, a cloud computing platform allowing users to run a wide range of geospatial analysis on Google's infrastructure. The platform simplifies geospatial analysis by providing users with several ways to interact with the platform and access a vast library of geospatial datasets for large scale spatial data processing. The online code editor in GEE is a web-based Integrated Development Environment IDE that allows writing and running JavaScript based codes that can be easily customized for multiple geospatial analysis through using various tools and client libraries. The wide range of pre-built algorithms and ready-to-use functions simplifies geospatial tasks such as image classification and developing and implementing geospatial models (Gorelick et al., 2017). The LULC classification and retrieval of spectral indices, LST and UTFVI were performed in GEE, while detailed accuracy assessment of land cover classifications and map formation and analysis was performed in ArcMap 10.8.

Google Earth Pro was used to obtain ground truth data of classes in the classified images to perform accuracy assessment. The correlation analysis between LST and spectral indices was performed by exporting relevant ArcMap data into Microsoft Excel for further evaluation. The questionnaire for the survey was generated using Google Forms that allowed analysis of results through pie and bar charts.

3.5. Land Use Land Cover Mapping

The supervised classification process was used in GEE to classify the satellite images for the study area into four main classes, namely water bodies, built-up, bare land, and vegetation. The first step was extracting the Area of Interest AOI and utilizing Landsat imagery from the image collections of Landsat 8 for the years 2023, 2018 and 2013, Landsat 5 for 2008 and Landsat 7 for 2003 respectively. A filter date was applied to retrieve images mainly of the summer months from March to July with less than 2% cloud cover for each year. A single composite image from the image collection was obtained through applying the `.median()` function. Approximately 300 to 600 sampling points were taken for each class using a stratified sampling approach and fed into the classifier.

Random Forest RF Classifier was used for this purpose, a popular Machine Learning ML algorithm that can be used for classification and regression analysis. RF is an ensemble method that builds on multiple decision trees to form a model and outputs the majority vote of individual trees. Figure 3 explains the working of a random forest classifier.

The sampling points were later split into a 70/30 ratio where 70% of the training samples were fed to the classifier in order to perform supervised machine learning-based classification. The remaining 30% of the samples were later used to validate and assess the accuracy of the classification. The classifier's optimal number of decision trees was set to 100 for maximum accuracy. The classified images were then exported to google drive from where they were downloaded and displayed in ArcMap.

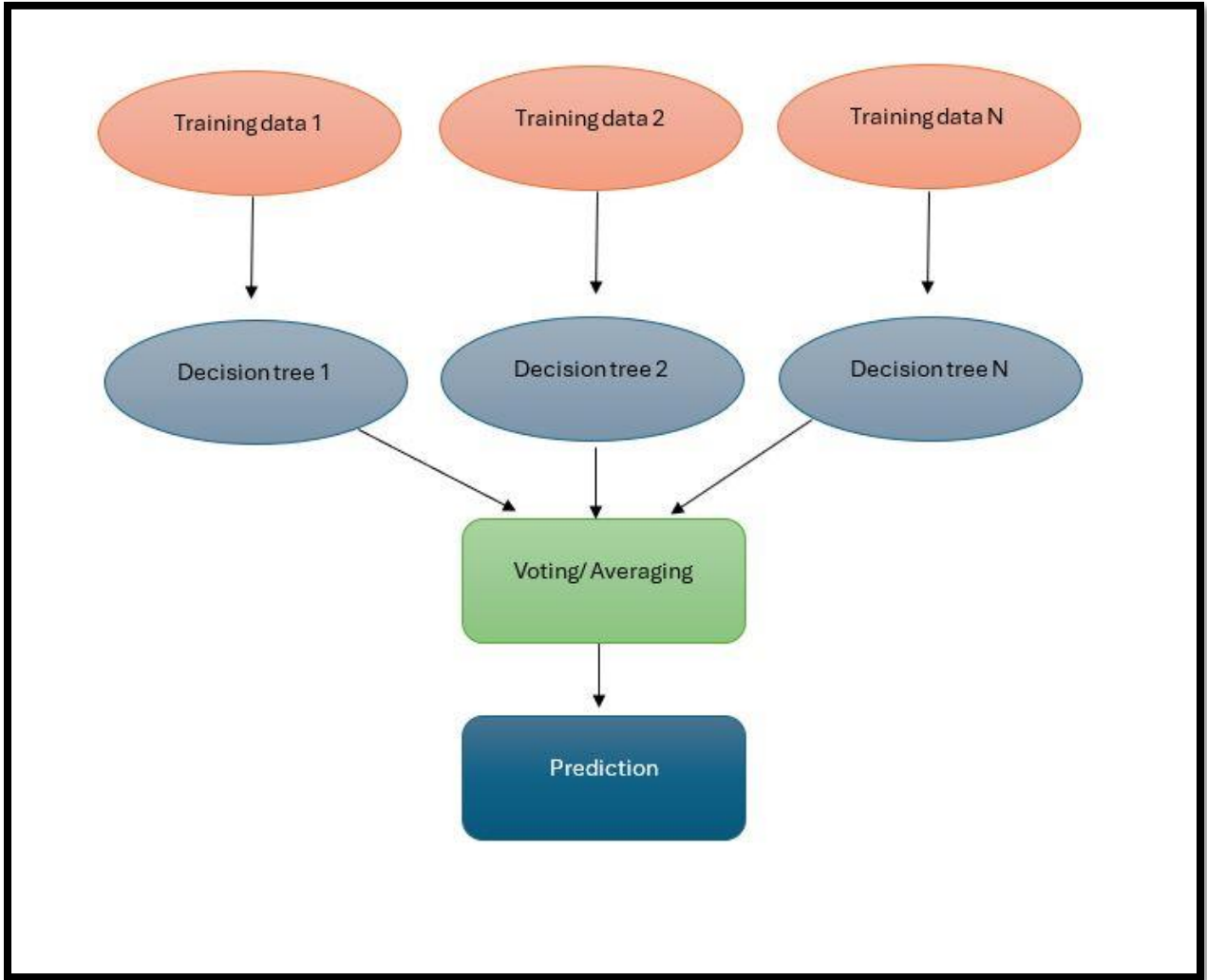


Figure 3. Random forest classifier.

3.6. Accuracy Assessment

A detailed accuracy assessment of the classified images was performed in ArcMap using two geoprocessing tools: creating accuracy assessment points and computing confusion matrix. A total of 200 points were taken using the stratified random sampling method where each class had number of points proportional to its relative area. The shapefile was then converted to KML file and exported to Google Earth Pro to obtain the ground truth data. The attribute table was updated through evaluating each point against the ground imagery to obtain ground truth data. The confusion matrix tables were then generated showing each classified image's user accuracy, producer accuracy and kappa coefficients. Overall accuracy is typically expressed as a percentage, with 100% accuracy indicating a perfect classification in which all reference sites were correctly identified. The term "Producer's Accuracy" refers to the map's accuracy as perceived by the map maker/producer. This shows how often real features on the ground are shown correctly on the classified map. The correctness of the map as seen by the user determines the likelihood that a class shown on the map will actually be present on the ground. This is known as user accuracy. An overall more than 70% accuracy is considered valid for a reliable classification. The Kappa Coefficient also evaluates the accuracy of a classification ranging from -1 to +1 with values close to +1 showing a reliable classification accuracy.

3.7. Retrieving Land Surface Temperature

Land surface temperature was calculated through using individual satellite images for each year. The date range was kept between march to august, essentially in the summer months and the average of each image was taken through the .median() function. Figure 4 shows a snippet of the code used for obtaining LST in GEE.

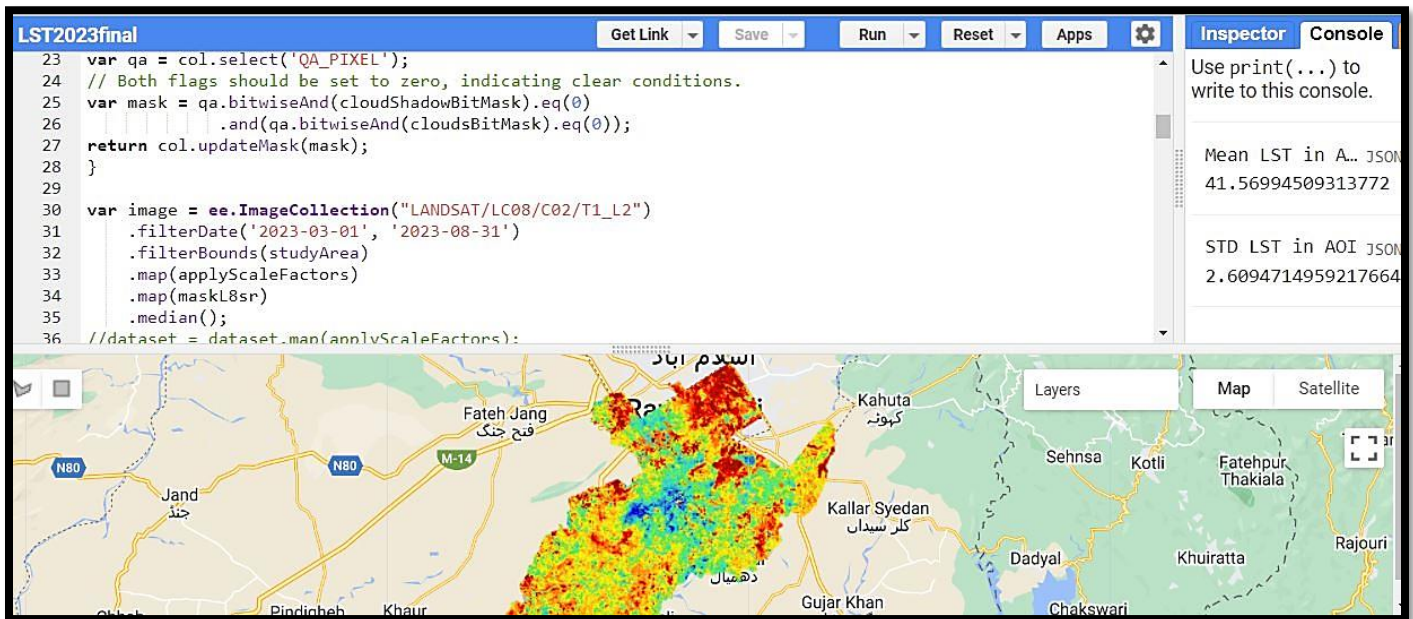


Figure 4. Code script for LST retrieval.

LST was calculated using the thermal bands ST_B6 for Landsat 5 and Landsat 7 and ST_B10 for Landsat 8 imageries.

3.7.1. Converting Digital Number (DN) values to Spectral Radiance

The thermal bands were used to convert digital number DN values to spectral radiance $L\lambda$ through using equation 1.

$$L\lambda = \frac{Lmax - Lmin}{QCALmax - QCALmin} * (QCAL - QCALmin) + Lmin \dots\dots\dots Eq 1$$

Where Lmax = maximum spectral radiance

Lmin = minimum spectral radiance

QCALmax = maximum digital number value (255)

QCAL min = minimum digital number value (1)

QCAL = digital number value of Band 6

3.7.2. Conversion to Top of Atmosphere (TOA) Radiance

The top of atmosphere radiance was calculated through using equation 2, (Waleed & Sajjad, 2022)

$$L\lambda = ML \times QCAL + AL \dots \dots \dots \text{Eq 2}$$

Where $L\lambda$ = TOA spectral radiance

ML = Band specific multiplicative rescaling factor

QCAL = digital number values of thermal band

AL= additive rescaling factor for the specific band

ML and AL values are retrieved from the MTL file of the imagery.

3.7.3. Conversion of Spectral Radiance $L\lambda$ to Brightness Temperature T_B

Equation 3 is used to convert spectral radiance to brightness temperature.

$$T_B = \frac{K2}{\ln\left(\frac{K1}{L\lambda} + 1\right)} \dots \dots \dots \text{Eq 3}$$

Where T_B = brightness temperature in kelvin

K2 & K1 = band specific constant values

(For Landsat 5: K2= 1260.56 and K1 = 607.76

For Landsat 7: K2 = 1282.71 and K1 = 666.09

For Landsat 8: K2 = 1321.0789 and K1 = 774.8853)

3.7.4. Calculating Spectral Emissivity

Spectral Emissivity is a crucial parameter in LST calculations and is the ratio of thermal radiation emitted by a surface at a specific wavelength to the thermal radiation emitted by a black body at the same wavelength and temperature. It requires calculation of PV (proportion of vegetation) that is calculated as shown in equation 4, (Mejbel Salih et al., 2018)

$$P_v = \left(\frac{NDVI - NDVI_{min}}{NDVI_{max} - NDVI_{min}} \right)^2 \dots\dots\dots Eq4$$

The Proportion of Vegetation is then used to calculate emissivity through the equation 5.

$$\varepsilon = 0.004P_v + 0.986 \dots\dots\dots Eq 5$$

3.7.5. Calculating Land Surface Temperature

The land surface temperature is calculated from the brightness temperature and emissivity using the equation 6,

$$LST = \frac{T_b}{1 + \left(\frac{\lambda \times T_b}{\rho} \right) \ln \varepsilon} - 273.15 \dots\dots\dots Eq 6$$

Where LST = surface temperature in Celsius

T_b = brightness temperature

λ = wavelength of emitted radiance

ρ = 1.438 × 10⁻² mK

ϵ = emissivity

3.8. Derivation of Spectral Indices

The spectral indices NDVI and NDBI were calculated using satellite imagery. NDVI is used to quantify vegetation greenness and is a useful tool to assess changes in plant health and understand vegetation density. NDVI is calculated as a ratio between the red and near infrared (NIR) bands of Landsat shown in equation 7.

$$\frac{NIR - RED}{NIR + RED} \dots \dots \dots \text{Eq 7}$$

For Landsat 4 – 7

$$\frac{Band\ 4 - Band\ 3}{Band\ 4 + Band\ 3} \dots \dots \dots \text{Eq 8}$$

For Landsat 8-9

$$\frac{Band\ 5 - Band\ 4}{Band\ 5 + Band\ 4} \dots \dots \dots \text{Eq 9}$$

NDVI range: -1 to +1

Low NDVI values (usually below 0.1): barren land, sand or snow

Moderate NDVI values (usually between 0.2 to 0.5): sparse vegetation, grasslands

High NDVI values (usually between 0.6 to 0.9): dense vegetation, crops at peak growth stage

NDBI uses Near Infrared (NIR) and Short Wave Infrared (SWIR) bands to emphasize the built up areas (Jothimani et al., 2021).

$$\frac{SWIR - NIR}{SWIR + NIR} \dots \dots \dots \text{Eq10}$$

For Landsat 4 – 7

$$\frac{\text{Band 5} - \text{Band 4}}{\text{Band 5} + \text{Band 4}} \dots \text{Eq 11}$$

For Landsat 8-9

$$\frac{\text{Band 6} - \text{Band 5}}{\text{Band 6} + \text{Band 5}} \dots \text{Eq 12}$$

NDBI range: -1 to +1

Low NDBI values (usually below 0.1): non urban areas

High NDBI values (usually between 0.6 to 0.9): urban areas

3.9. Correlating Indices with LST

A random points tool was used to create specific random point features to evaluate the relationship between LST and spectral indices NDVI and NDBI. About 500 random points were generated and the multi values tool was used in ArcMap to extract the values of LST, NDVI and NDBI for 2003, 2008, 2013, 2018 and 2023. The correlation analysis was performed in Microsoft Excel and scatterplots were generated to visualize the relationship between LST and NDVI and LST and NDBI respectively.

3.10. UHI Analysis through Calculating UTFVI

In this study, urban heat island effect has been quantified using the Urban Thermal Field Variance Index, among the most widely used thermal comfort indices measuring the thermal variance within an urban area. UTFVI maps can also assist in identifying the hot spots within a city with high-temperature values compared to the surrounding areas. The UTFVI was also obtained from GEE through using the following formula,

$$\text{UTFVI} = \frac{T_s - T_m}{T_s} \dots \dots \dots \text{Eq 13}$$

Where T_s = calculated LST

T_m = mean LST value

The UTFVI values are mainly computed for the summer season using the LST images generated for the years 2003, 2008, 2013, 2018 and 2023. The UTFVI values were further categorized into six classes, signifying the intensity of the urban heat island effect according to the categories shown in table 2 (Waleed et al., 2023).

Table 2. The UTFVI reference values.

UTFVI threshold values	UHI intensity
<0.005	Least significant heat island effect
0.005 - 0.015	Weak urban heat island effect
0.015 – 0.025	Moderate urban heat island effect
0.025 – 0.035	Strong urban heat island effect
UTFVI > 0.035	Very strong urban heat island effect

Low UTFVI values often occur in areas with vegetation or less built up while high UTFVI values are consistent with the areas having a strong UHI effect such as intensely developed built up areas or bare land.

3.11. Survey Conduction

An online survey was conducted through Google Forms to assess the impacts of land use land cover changes and increase in land surface temperature and urban heat island formation on the

socio-economic factors in Rawalpindi. The survey was conducted through a brief questionnaire, and it was ensured that no personally identifiable information was collected from the participants. The questionnaire included 11 main questions apart from the general questions of age, gender, education level and employment level. The questions were framed to assess the general perception about the temperature changes in Rawalpindi, the perceived causes of rising temperature and the intensity of heat during the summer months. The next few questions were developed to assess the population health in relevance to heat related illnesses. The questionnaire also assessed factors regarding resource and energy consumption such as hike in electricity prices, along with experiencing power outages and water shortages. Lastly the participants were asked for comments and suggestions regarding mitigating the impacts of rising temperature in the city and some of those recommendations are added in the mitigation strategies after careful evaluation.

RESULTS AND DISCUSSION

4.1. Land Use Land Cover

Land use land cover was obtained using satellite images from 2003, 2008, 2013, 2018, and 2023, which were classified in Google Earth Engine through the Random Forest Classifier. Four classes, including waterbodies, built up, bare land and vegetation were made and approximately 300 to 600 training points were taken for each class using a stratified sampling approach. The points were fed into the classifier to perform machine learning based supervised classification. The images were then exported to Google Drive and downloaded to display the results and formulate maps in ArcMap. Figure 5 shows the combined images of the training points selected for classification in GEE. Figures 6-10 show the individual classifications for the years 2003, 2008, 2013, 2018 and 2023. The accuracy assessments for the classified images were performed using ArcMap and Google Earth Pro as ground truth data for the accuracy points, which were obtained from Google Earth imagery for the particular year. The overall accuracies are 83.5%, 77.9%, 80%, 80% and 85.4% for the years 2003, 2008, 2013, 2018, and 2023 respectively. Kappa coefficients are 0.72, 0.68, 0.73, 0.70, and 0.79 for the years 2003, 2008, 2013, 2018 and 2023 respectively. Kappa statistics of less than 0.2 signify poor agreement, 0.2 to 0.4 signify fair agreement, 0.4 to 0.6 signify moderate agreement while 0.6 to 0.8 represent substantial agreement (Bernet et al., 2019). The kappa values for classifications in this study are between 0.6 to 0.8, that signify a substantial agreement and reliable classification values. It is observed from the results that an increasing trend is seen particularly in the built-up class. The tables 3-7 show detailed confusion matrices for the classification accuracies of respective years.

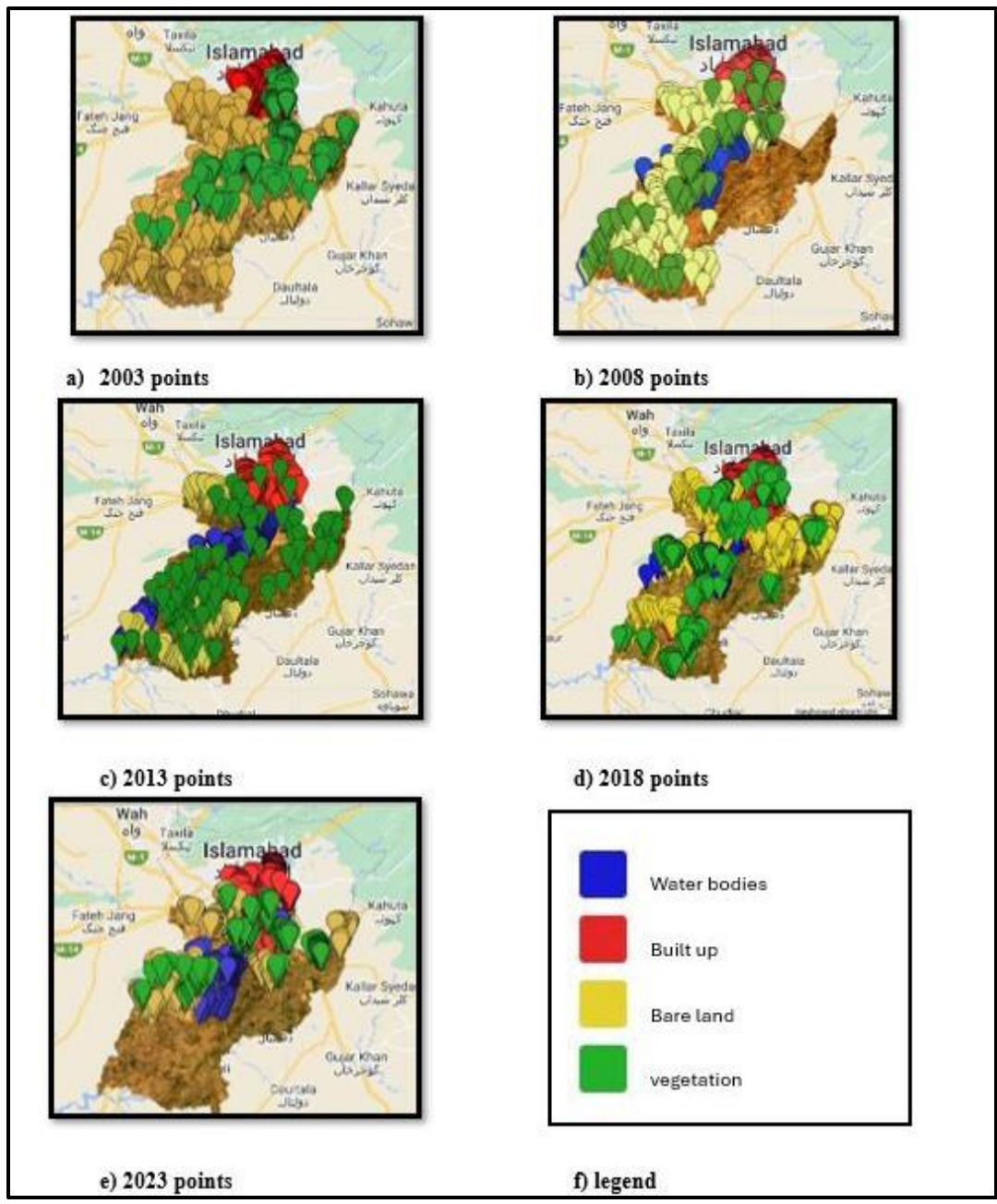


Figure 5. Training points for supervised classification.

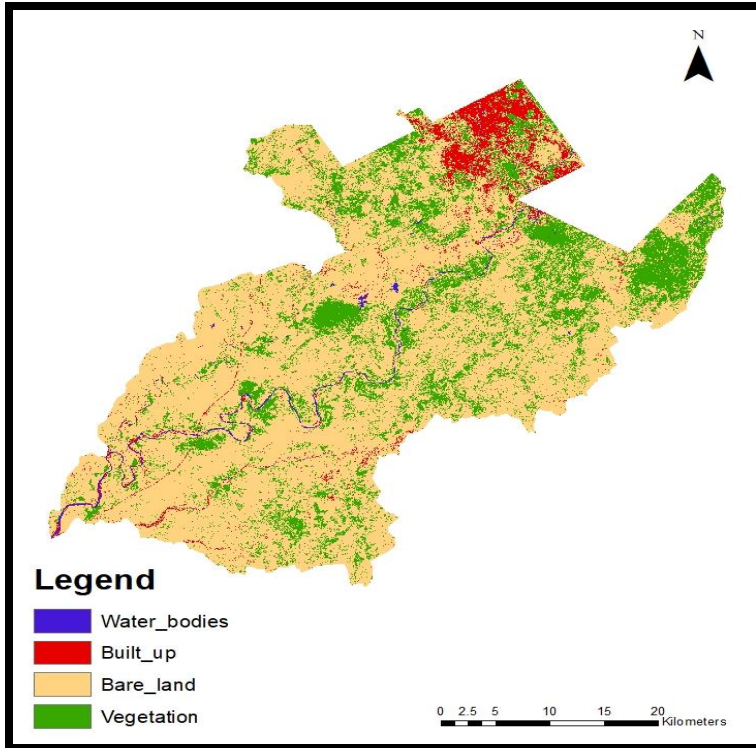


Figure 6. The study area land use/ land cover classification for the year 2003

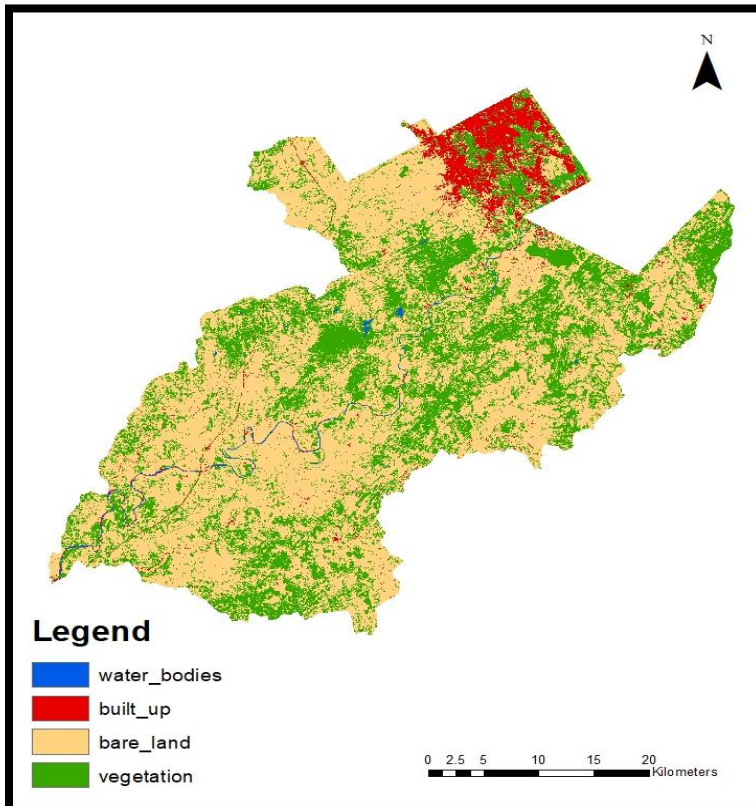


Figure 7. The study area land use/ land cover classification for the year 2008

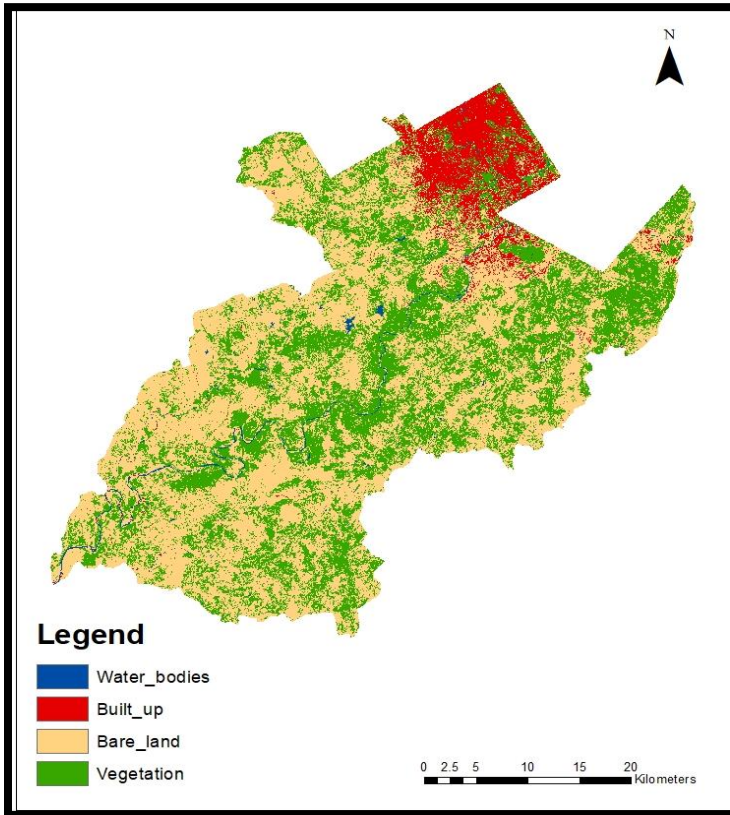


Figure 8. The study area land use/ land cover classification for the year 2013

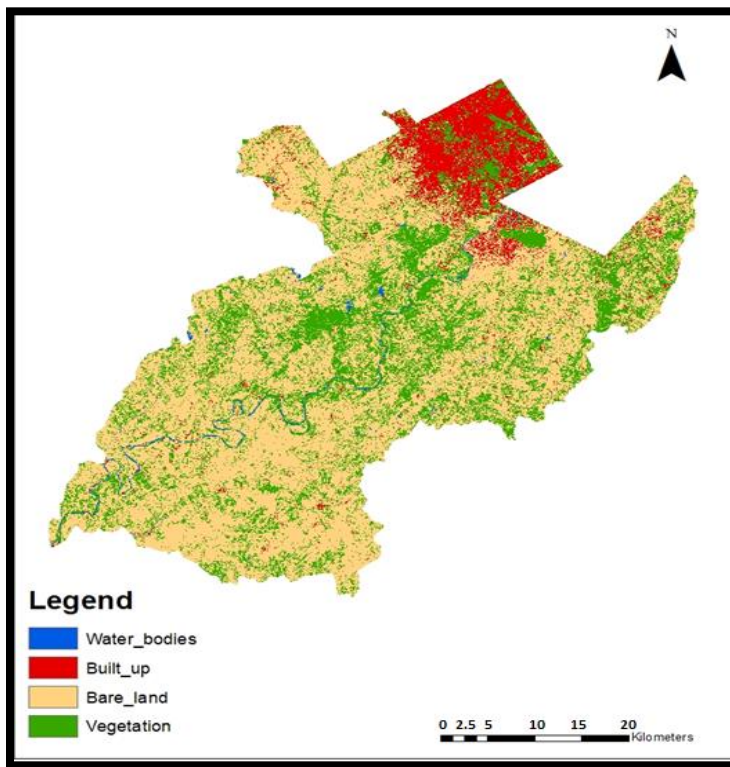


Figure 9. The study area land use/land cover classification for the year 2018

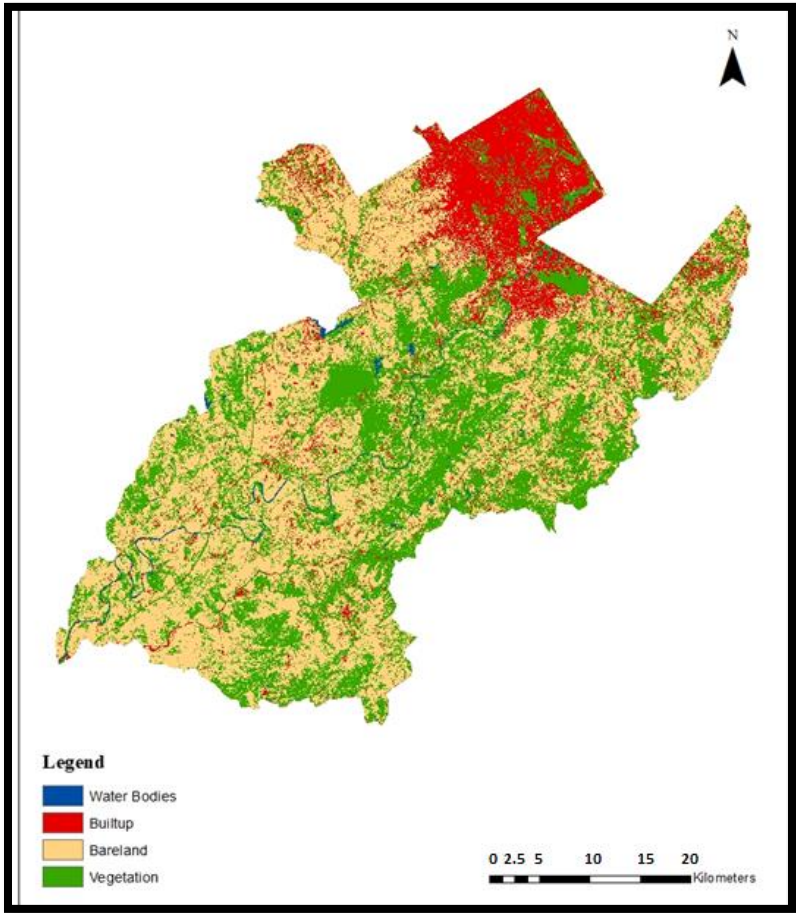


Figure 10. The study area land use/ land cover classification for the year 2023

Table 3. Overall accuracy assessment of classified image (2003).

Classes	Water bodies	Built up	Bare land	Vegetation	Total	User accuracy	Kappa
Water bodies	7	0	3	0	10	0.7	
Built up	0	6	4	0	10	0.6	
Bare land	0	0	36	0	36	1	
Vegetation	0	0	4	7	11	0.64	
Total	7	6	47	7	67	0	
Producer accuracy	1	1	0.77	1	0	0.835	
Kappa							0.72
Overall accuracy	83.5%						

Table 4. Overall accuracy assessment of classified image (2008).

Classes	Water bodies	Built up	Bare land	Vegetation	Total	User accuracy	Kappa
Water bodies	7	0	3	0	10	0.7	
Built up	0	8	2	0	10	0.8	
Bare land	1	1	24	5	31	0.77	
Vegetation	0	0	3	14	17	0.82	
Total	8	9	32	19	68	0	
Producer accuracy	0.88	0.89	0.75	0.74	0	0.779	
Kappa							0.68
Overall accuracy	77.9%						

Table 5. Overall accuracy assessment of classified image (2013).

Classes	Water bodies	Built up	Bare land	Vegetation	Total	User accuracy	Kappa
Water bodies	10	0	0	0	10	1	
Built up	0	10	0	0	10	1	
Bare land	0	1	9	0	10	0.9	
Vegetation	0	0	7	3	10	0.3	
Total	10	11	16	3	40	0	
Producer accuracy	1	0.91	0.56	1	0	0.8	
Kappa							0.73
Overall accuracy	80%						

Table 6. Overall accuracy assessment of classified image (2018).

Classes	Water bodies	Built up	Bare land	Vegetation	Total	User accuracy	Kappa
Water bodies	6	0	3	1	10	0.6	
Built up	0	9	1	0	10	0.9	
Bare land	0	2	26	3	31	0.84	
Vegetation	0	1	2	11	14	0.78	
Total	6	12	32	15	65	0	
Producer accuracy	1	0.75	0.81	0.73	0	0.8	
Kappa							0.70
Overall Accuracy	80%						

Table 7. Overall accuracy assessment of classified image (2023).

Classes	Water bodies	Built up	Bare land	Vegetation	Total	User accuracy	Kappa
Water bodies	6	0	2	2	10	0.6	
Built up	0	10	0	0	10	1	
Bare land	0	1	22	1	24	0.92	
Vegetation	0	0	3	15	18	0.83	
Total	6	11	27	18	62	0	
Producer accuracy	1	0.91	0.81	0.83	0	0.854	
Kappa							0.79
Overall Accuracy	85.4%						

4.1.1 Land Use Land Cover Change Detection

The classified images reveal that significant urban expansion has occurred in Rawalpindi over a time span of 20 years from 2003 to 2023. With urban sprawl and development of new societies, the built-up area has increased significantly and has become denser with increased population. The built-up area increased from 74.5 Km² in 2003 to 227.7 Km² in 2023 with an overall increase of 206% in area. This tremendous urban expansion and huge human influx can be attributed to a high growth and migration rate as people from rural areas and underdeveloped cities migrate to developed cities such as Rawalpindi and Islamabad in search of education, jobs, business purposes and other opportunities and resources. Due to this rising urban expansion, and consequent rise of impervious surfaces, the temperature in the city is rising by the day. Table 8 shows the change in land use land cover classes over the years while the overall change is illustrated in figure 11.

Table 8. LULC change (Km²)

Year	Built-up	Vegetation	Water	Bare land
2003	74.5	362.92	14.25	1191.57
2008	79.04	544.32	9.02	1010.85
2013	115.64	622.57	15.13	885.35
2018	135.01	456.66	13.13	1038.43
2023	227.71	590.38	16.97	808.19
Change from 2003 to 2023 (Km²)	153.2	227.08	2	-383.38

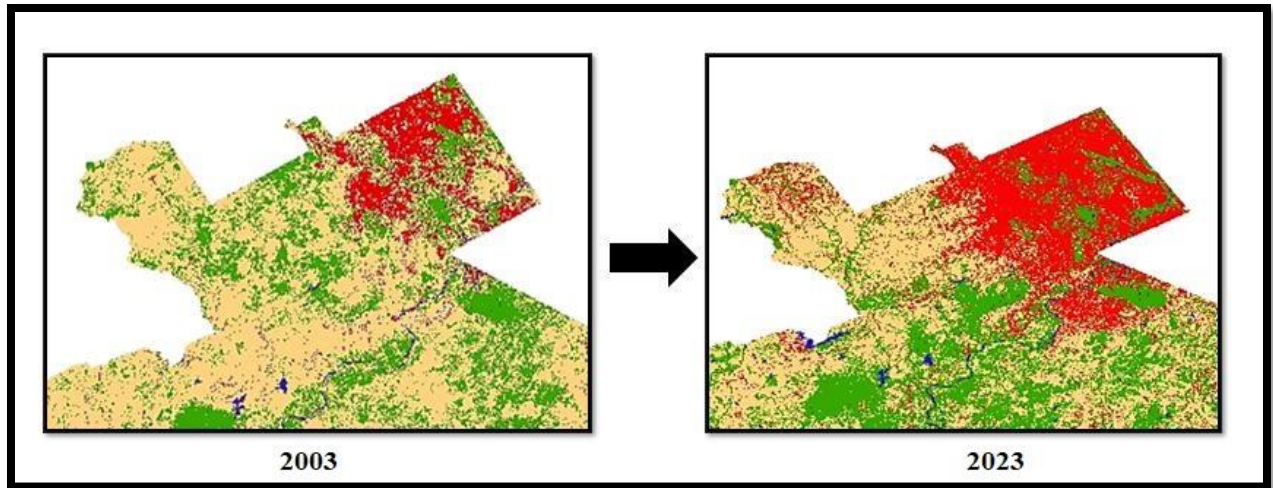


Figure 11. The study area built-up increase 2003 to 2023

4.2. Land Surface Temperature Retrieval

The Land surface temperature was calculated in Google Earth Engine and the LST images obtained are consistent with the built-up area values obtained from the classified images. The mean LST temperatures have been obtained for the built-up area values particularly for each year through obtaining zonal statistics adding LST and classified images as inputs. The results generated minimum, maximum and mean LST values and area values for each class: water bodies, built up, bare land, and vegetation. The results in table 9 show that the mean LST values are 34 °C, 33°C, 35°C, 37°C and 39°C for the years 2003, 2008, 2013, 2018 and 2023 respectively. The mean LST values have been increasing throughout the years and this increase is mainly attributed to the rapid urban expansion and increase in built up areas. Temperature is seen to be the highest in 2023 when the built-up area reached 227.7 square kilometers, minimum LST is found to be 29 °C, while maximum LST is found to be 44°C in the built-up area. The study mainly focused on the relationship between LST and built-up expansion due to which the temporal change in LST has mainly been analyzed along with increase in built up areas and the other classes namely water

bodies and bare land have been excluded. The LST and built-up area have increased parallel to each other from 2003 to 2023 that is mainly due to the high heat absorption capacity of impervious surfaces, and the emitted radiation is then trapped in the atmosphere due to the enhanced greenhouse effect, thus increasing both land and air temperatures in urban areas. Figure 12-16 illustrate the land surface temperature maps for the respective study years.

4.3. Correlation of Spectral Indices with LST

The spectral indices maps were also obtained from Google Earth Engine through using the NIR and Red bands for NDVI and NIR and SWIR bands for NDBI. About 500 random points were generated and ‘extract multi values tool’ was used in ArcMap to extract the values of LST, NDVI and NDBI for the years 2003, 2008, 2013, 2018 and 2023. NDVI and LST are negatively correlated with each other as the areas with high greenness and vegetation have low LST and vice versa, while NDBI and LST are positively correlated with each other as the areas with high built-up density experienced higher land surface temperatures as compared to areas with lower built-up density. Table 10 shows a negative correlation between NDVI and LST while Table 11 shows a positive correlation between NDBI and LST.

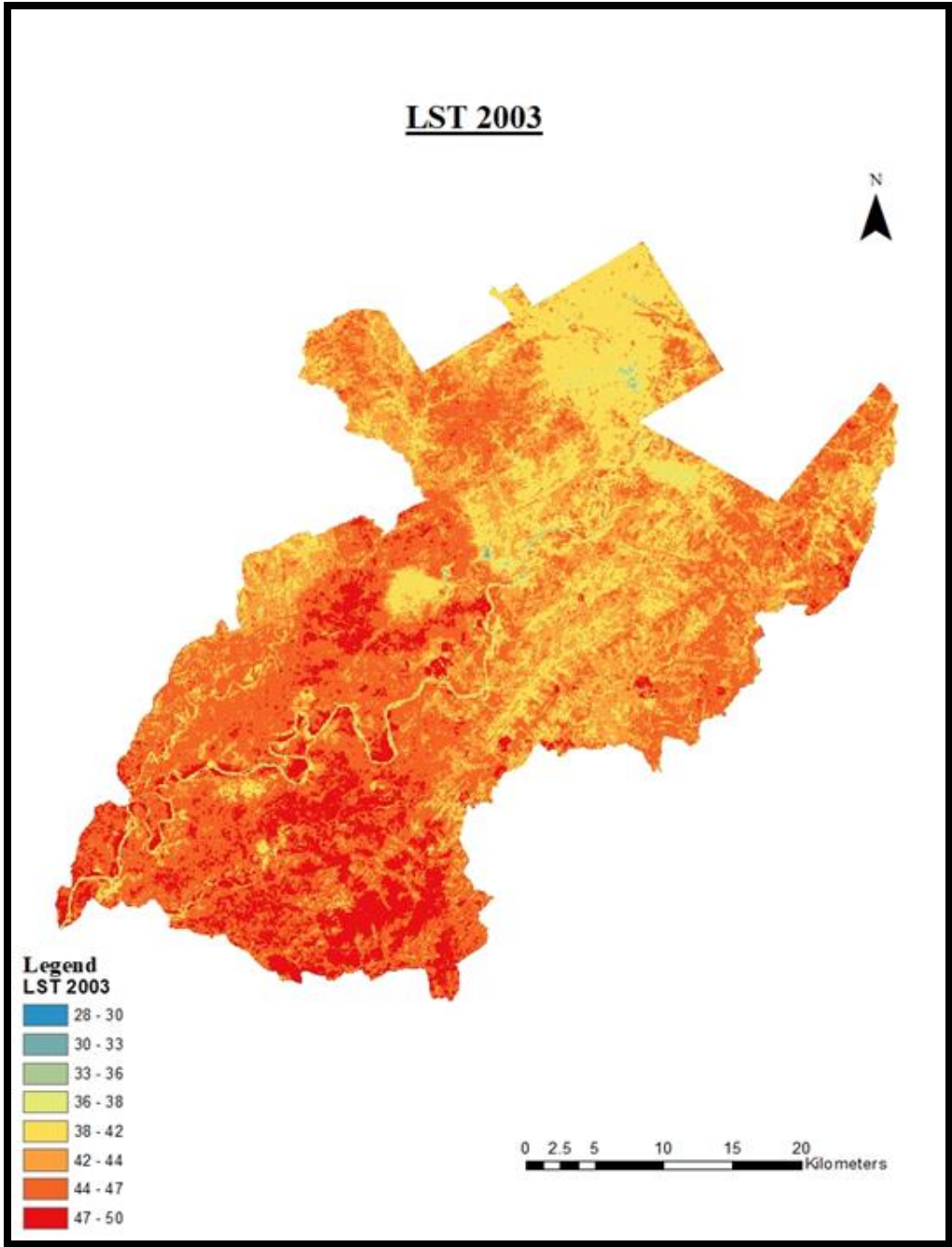


Figure 12. The study area land surface temperature of 2003

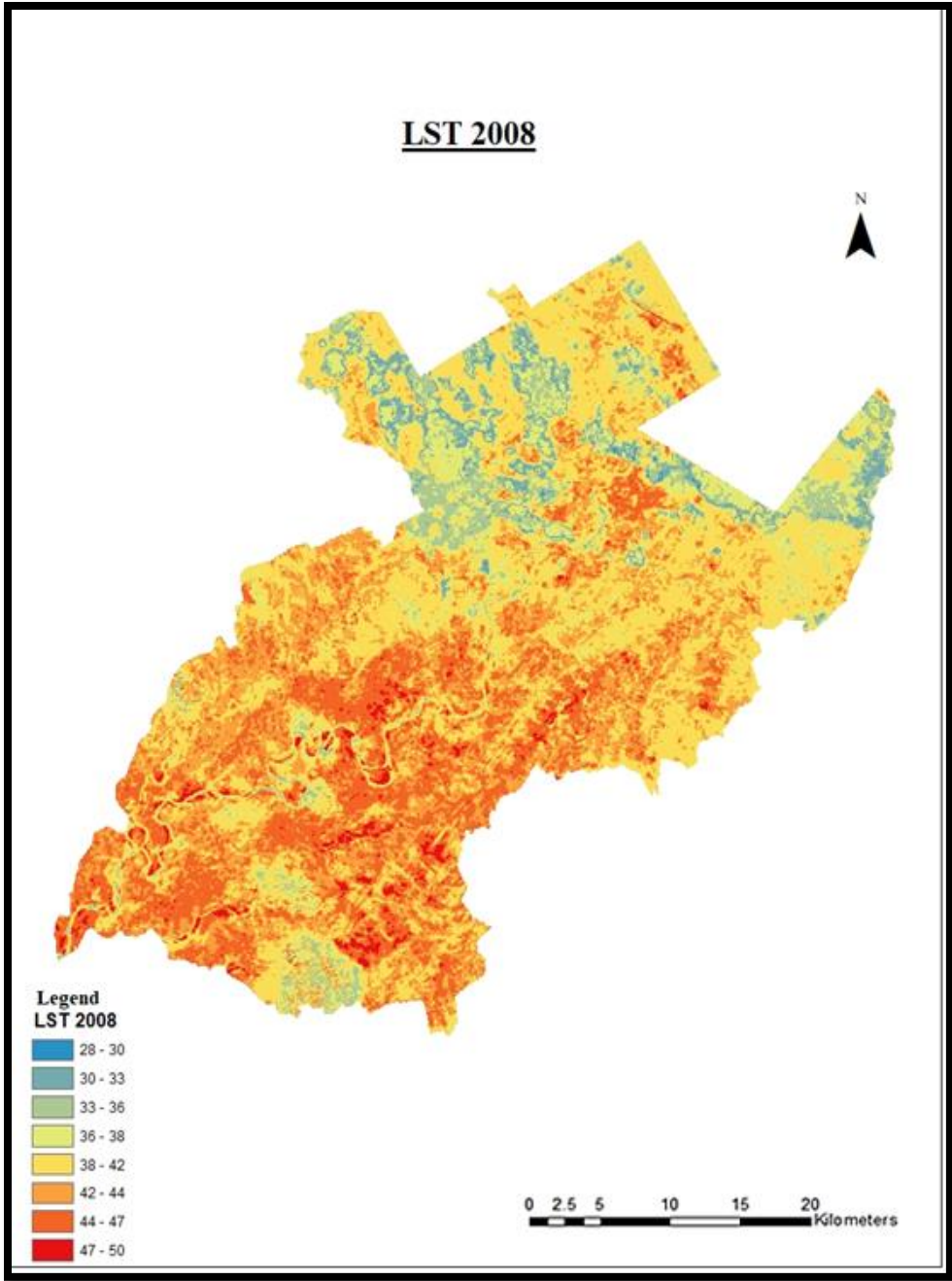


Figure 13. The study area land surface temperature of 2008

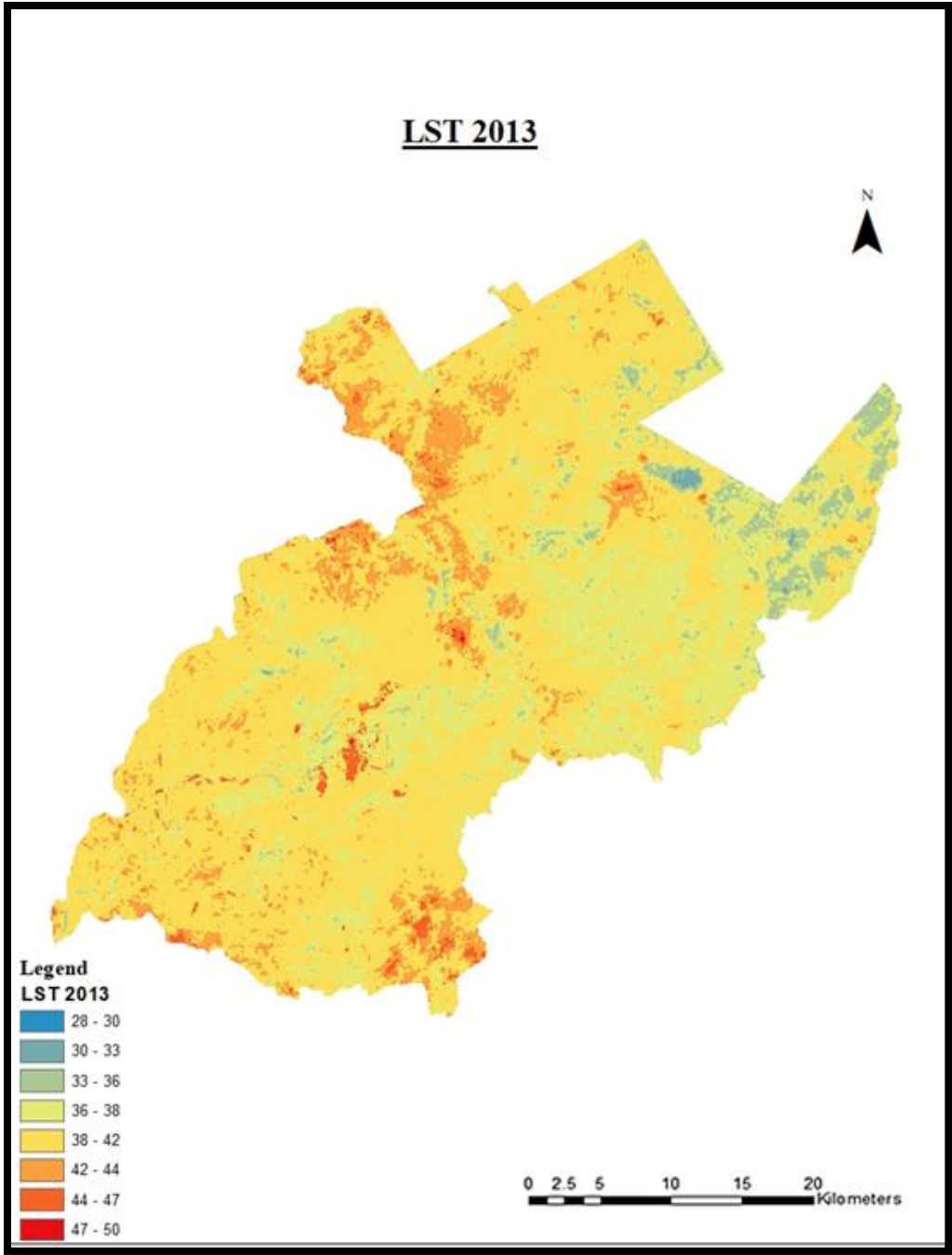


Figure 14. The study area land surface temperature of 2013

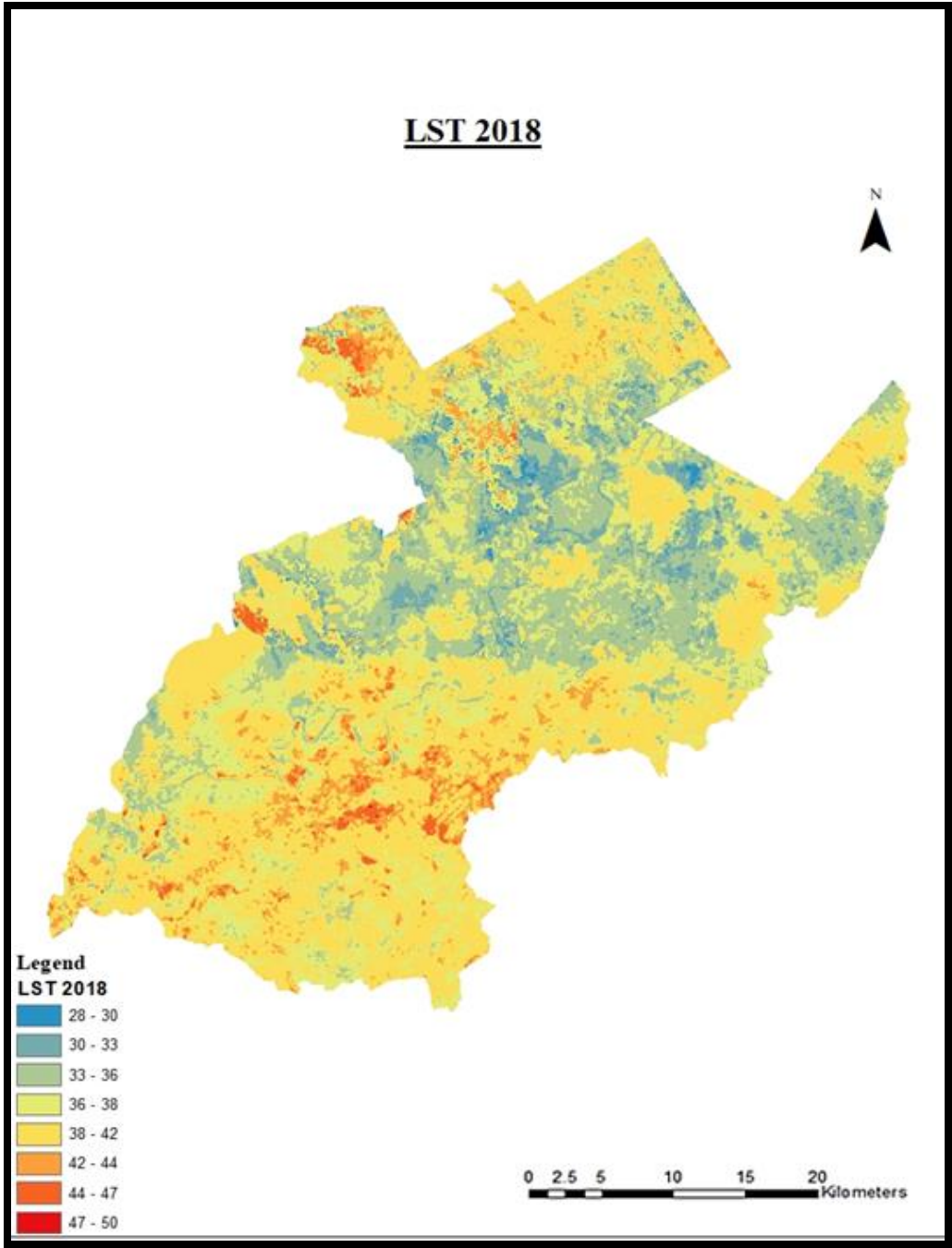


Figure 15. The study area land surface temperature of 2018

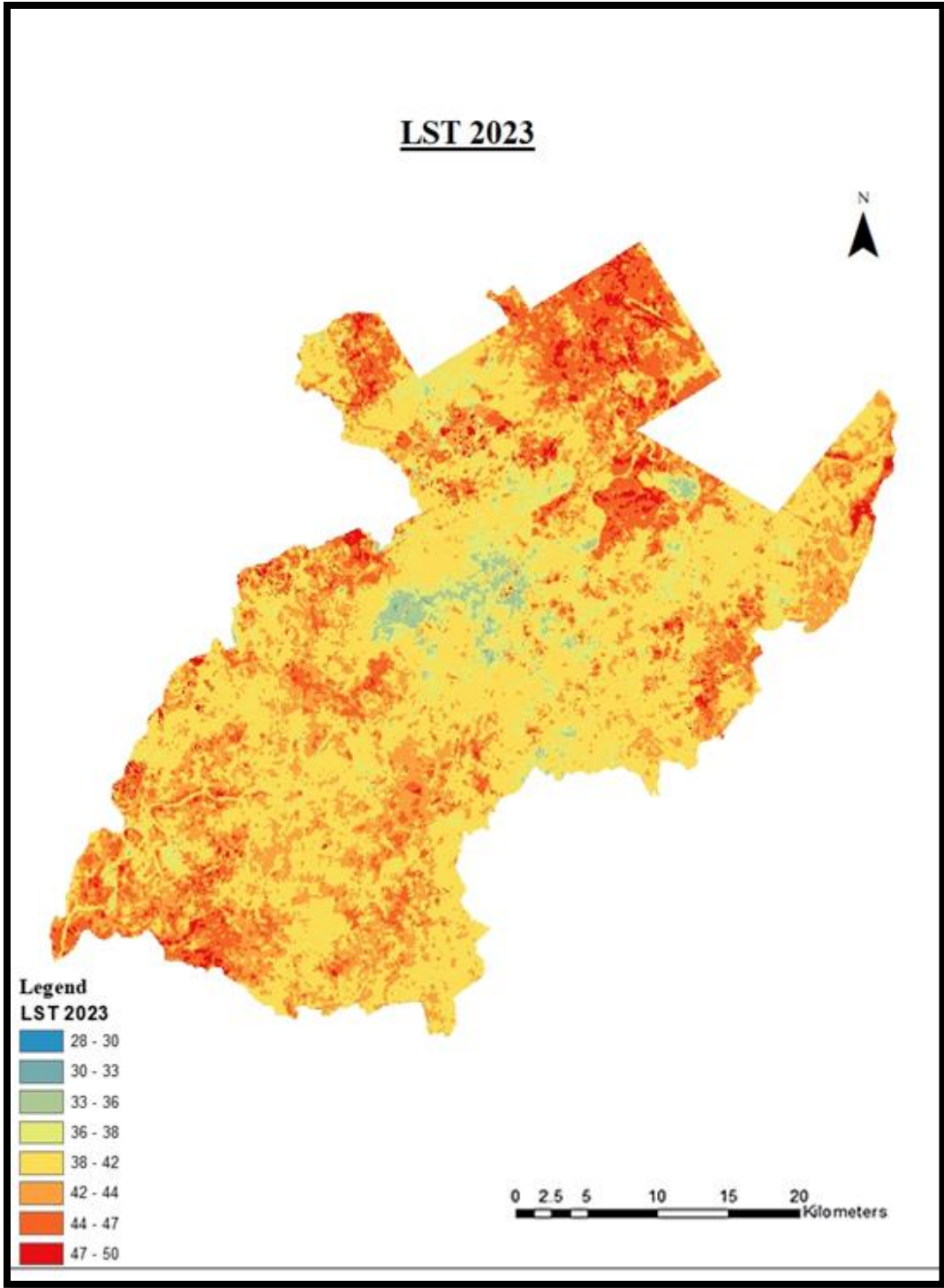


Figure 16. The study area land surface temperature of 2023

Table 9. Temporal change in LST and built-up.

Year	Built up area (km ²)	Min LST (°C)	Max LST (°C)	Mean LST (°C)
2003	74.5	28	40	34
2008	79.04	26	38	33
2013	115.64	31	40	35
2018	135.01	31	43	37
2023	227.71	29	44	39

Table 10. Correlation of NDVI with LST

	NDVI2003	NDVI2008	NDVI2013	NDVI2018	NDVI2023
LST2003	-0.398				
LST2008	-0.254	-0.864			
LST2013	-0.182	-0.178	-0.759		
LST2018	-0.175	-0.477	-0.029	-0.421	
LST2023	-0.153	-0.514	-0.081	-0.446	-0.268

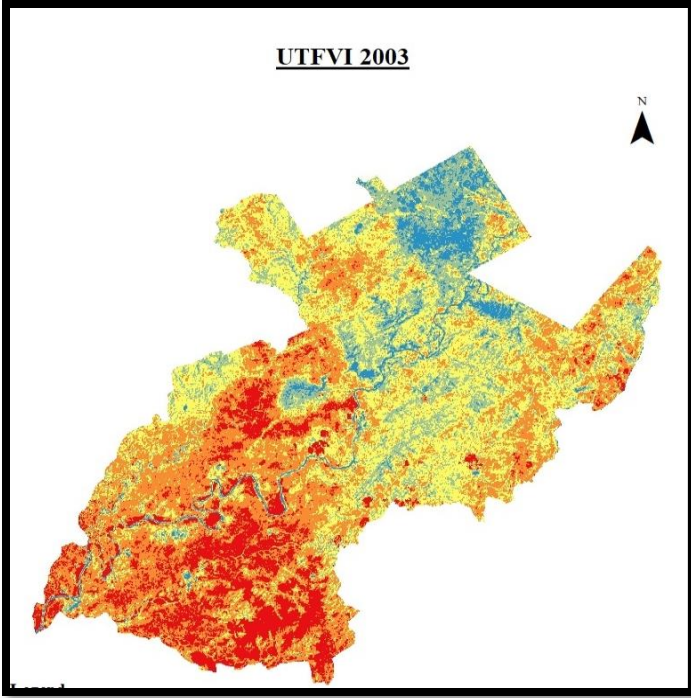
Table 11. Correlation of NDBI with LST.

	NDBI2003	NDBI2008	NDBI2013	NDBI2018	NDBI2023
LST2003	0.139082				
LST2008	0.11014	0.39119			
LST2013	0.052631	0.02343	0.217966		
LST2018	0.03288	0.01814	0.05608	0.366678	
LST2023	0.034889	0.019698	0.091957	0.00727	0.37913

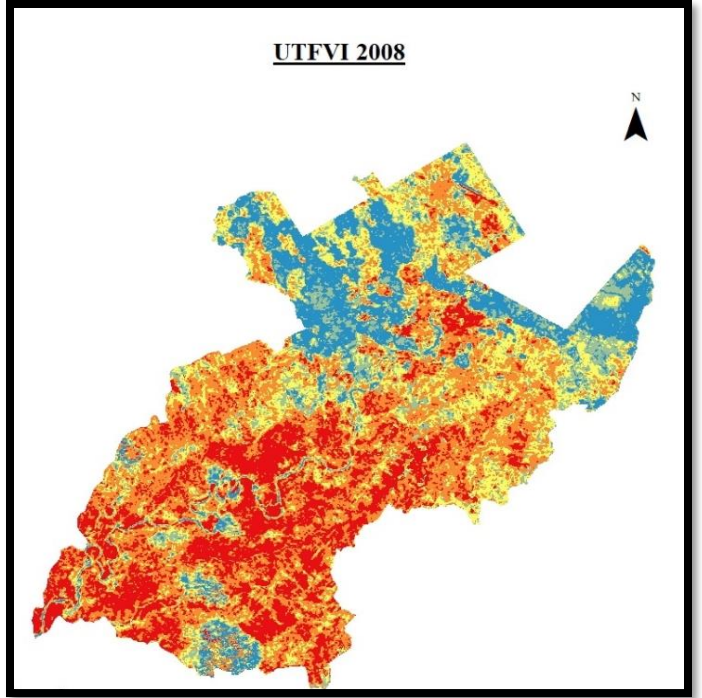
4.4. Urban Thermal Field Variance Index

Figure 17 shows the Urban Thermal Field Variance Index maps that are categorized according to the threshold values showing the strength of UTFVI. The UTFVI intensity is seen high in barren land as bare soil absorbs more heat, however, the UTFVI intensity of concern is in the built-up areas where due to urban expansion, the UHI effect has become stronger over the years from 2003 to 2023. Areas showing low UTFVI strength in 2003 have been converted to those with strong and severe UTFVI effect in 2023. This increase in UTFVI is associated with higher Land Surface Temperatures (LST) in many regions of the city, owing to the expansion of built-up areas, reduced vegetation cover, and the presence of heat-absorbing materials such as concrete and asphalt. The high UTFVI values emphasize the severity of thermal variance, with certain areas experiencing significantly greater temperatures than their surroundings. These raised LST levels increase energy consumption, cooling expenses, and health hazards, especially during heatwaves. The maps depict that in a time span of 20 years, majority of the built-up area in the main Rawalpindi city has been converted to strong/severe UTFVI zone that experience a high urban heat island effect. The majority of the built-up areas in Rawalpindi lack significant green spaces and are densely populated with heavy traffic and some experiencing high commercial and industrial activities. Densely populated areas such as Raja Bazar, Saddar, Waris Khan, Gawal Mandi, Pir Wadhai, Satellite town and other industrialized areas experience high UHI effect as compared to their surrounding areas with less urban cover.

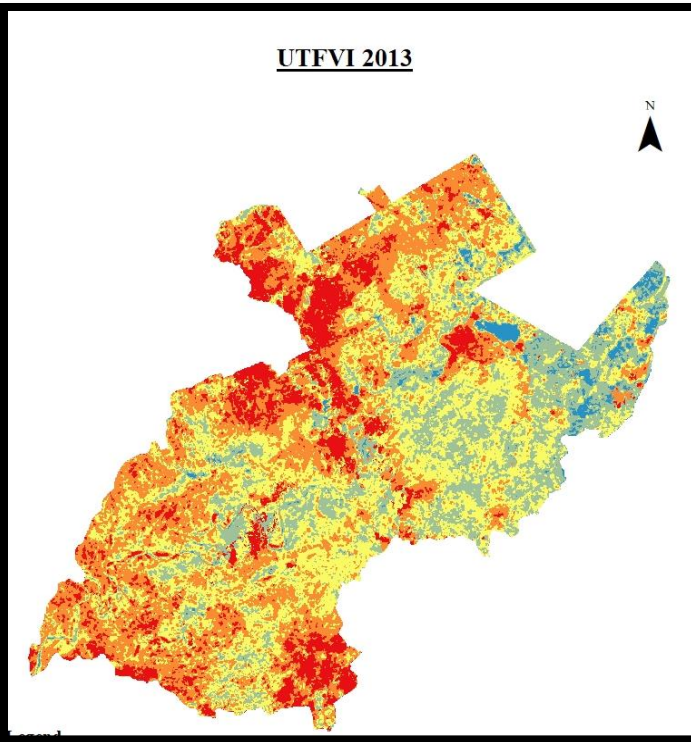
UTFVI 2003



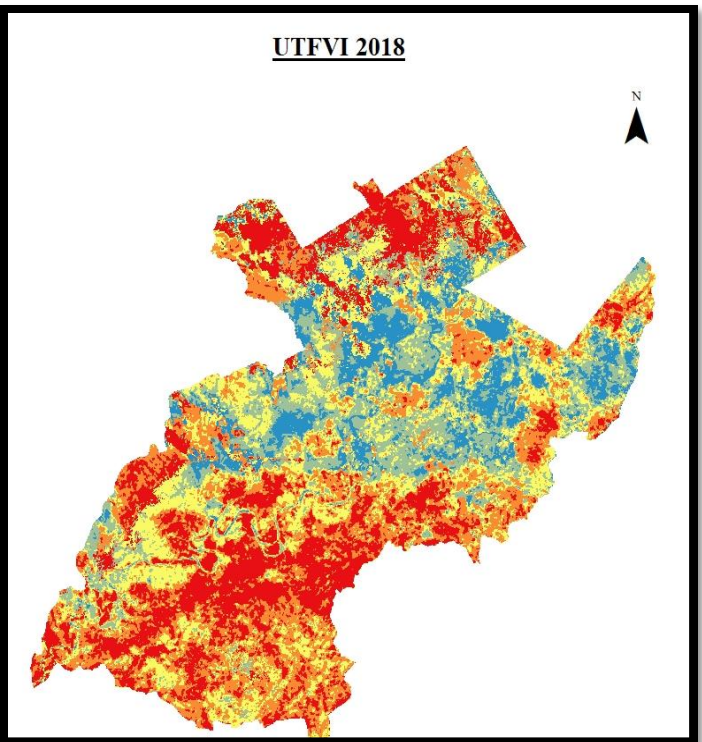
UTFVI 2008



UTFVI 2013



UTFVI 2018



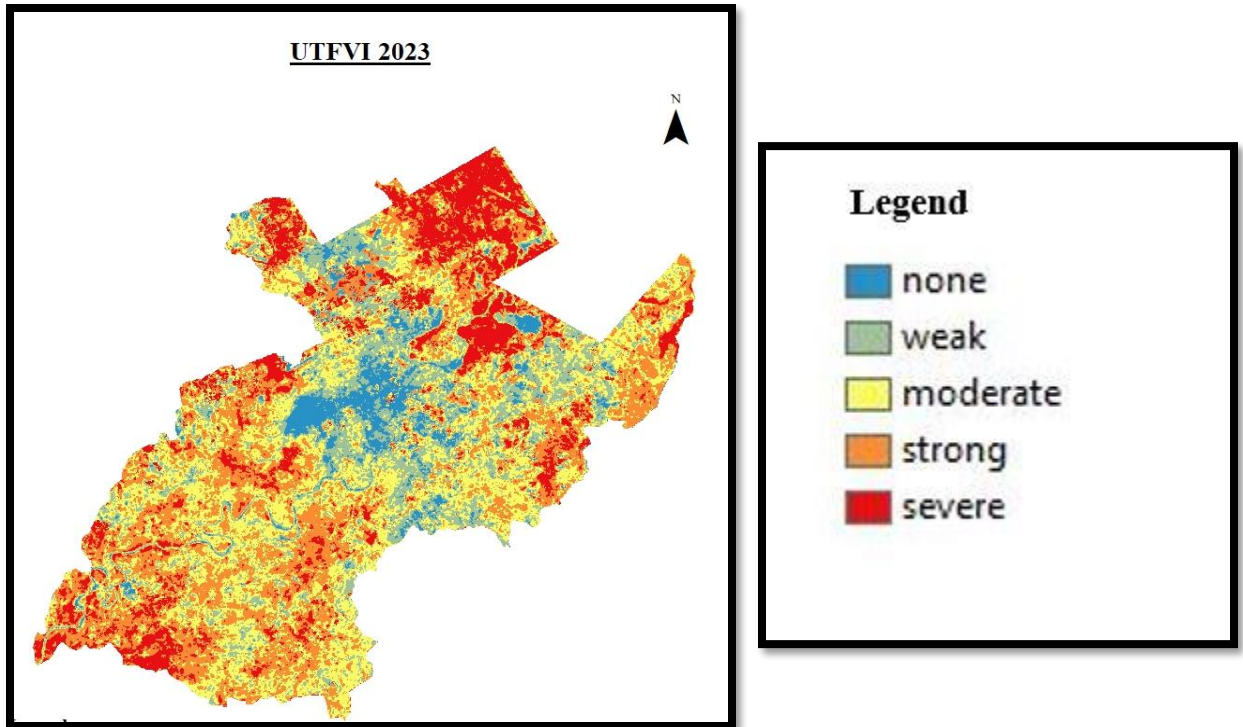


Figure 17. The study area UTFVI maps for years 2003, 2008, 2013, 2018, and 2023

4.5. Results from Survey Conduction

A brief survey was conducted through google forms to analyze the impact of rise in temperature and urban heat island formation in built up areas of Rawalpindi. The survey results indicated that the temperature levels in the study area have risen as about 77% of respondents believed that the temperature in Rawalpindi has become significantly warmer in the past 10 to 15 years. Moreover, about 44% of the respondents believed that the temperature of Rawalpindi city was significantly warmer than that of the surrounding areas, such as Islamabad, as a major temperature change is witnessed between the twin cities.

The figures 18-22 present some of the questions asked for the survey and their relevant responses from the participants.

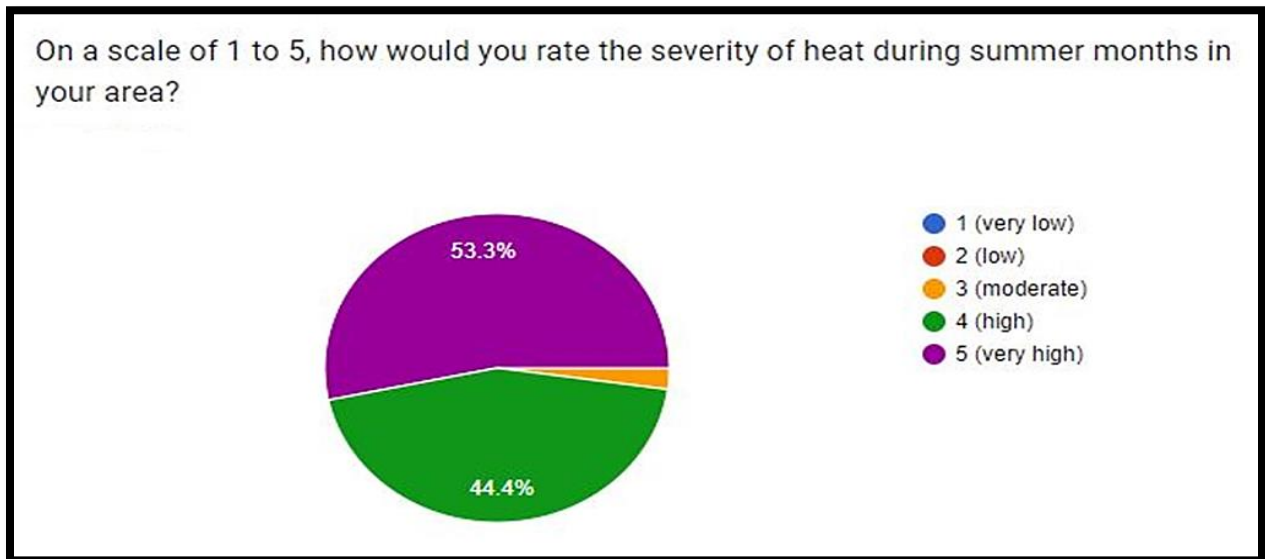


Figure 18. Survey question 1 response

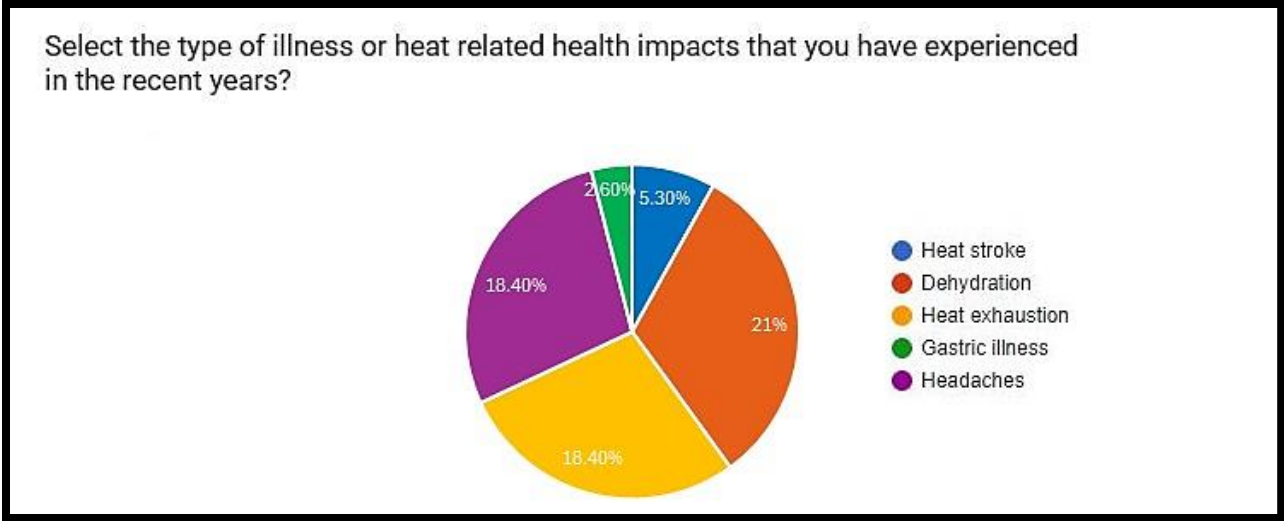


Figure 19. Survey question 2 response

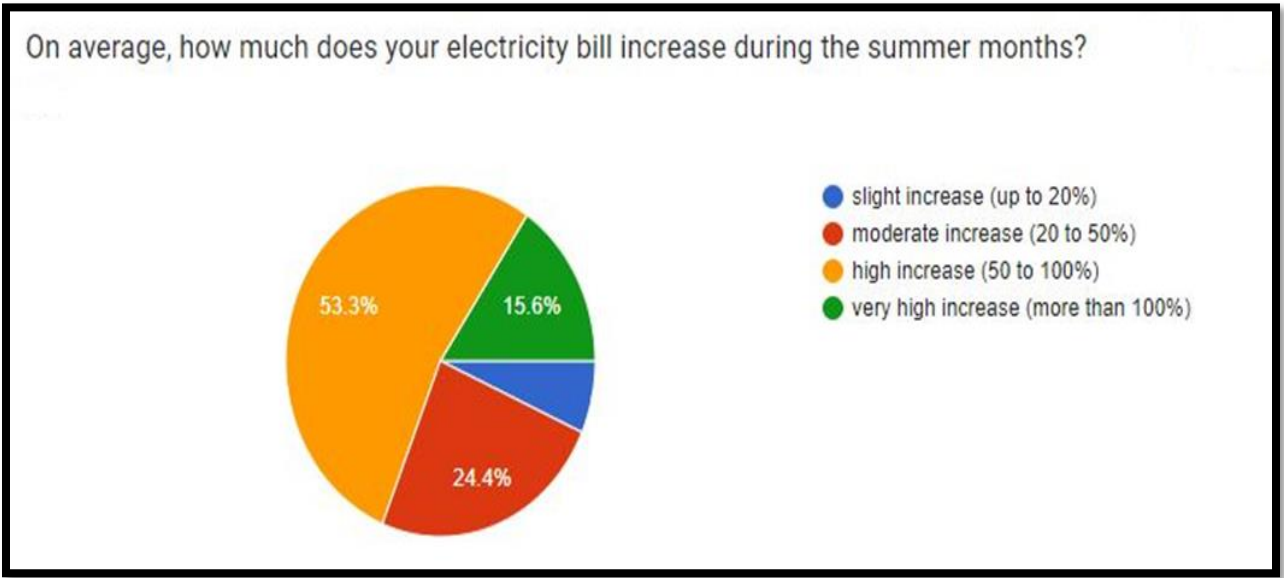


Figure 20. Survey question 3 response

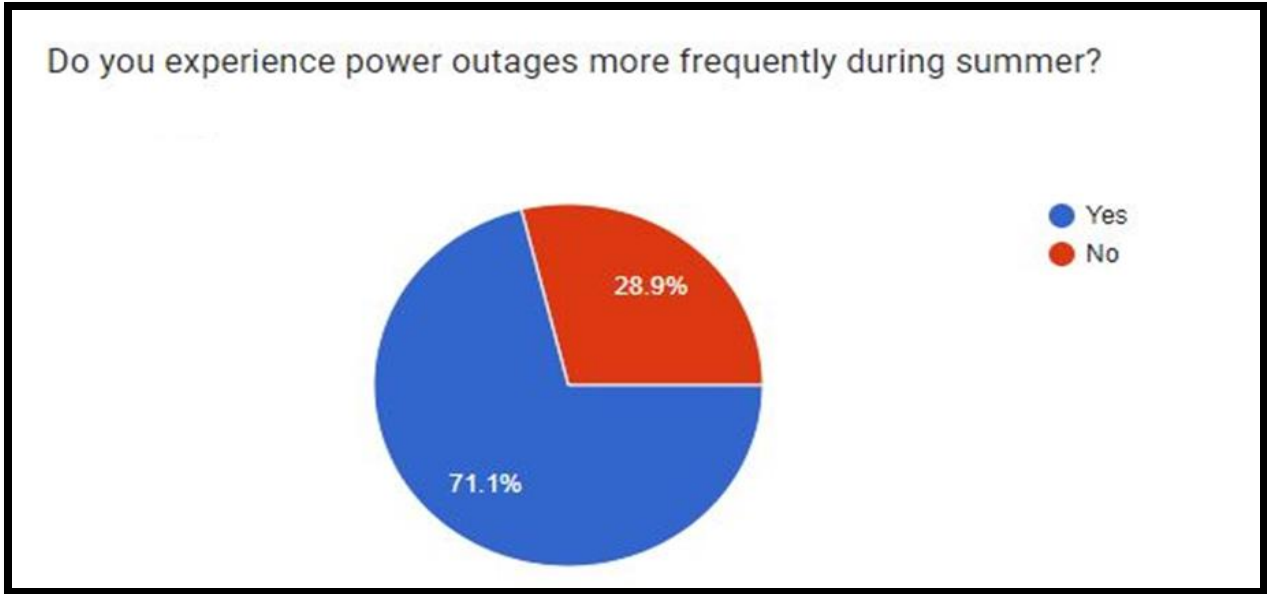


Figure 21. Survey question 4 response

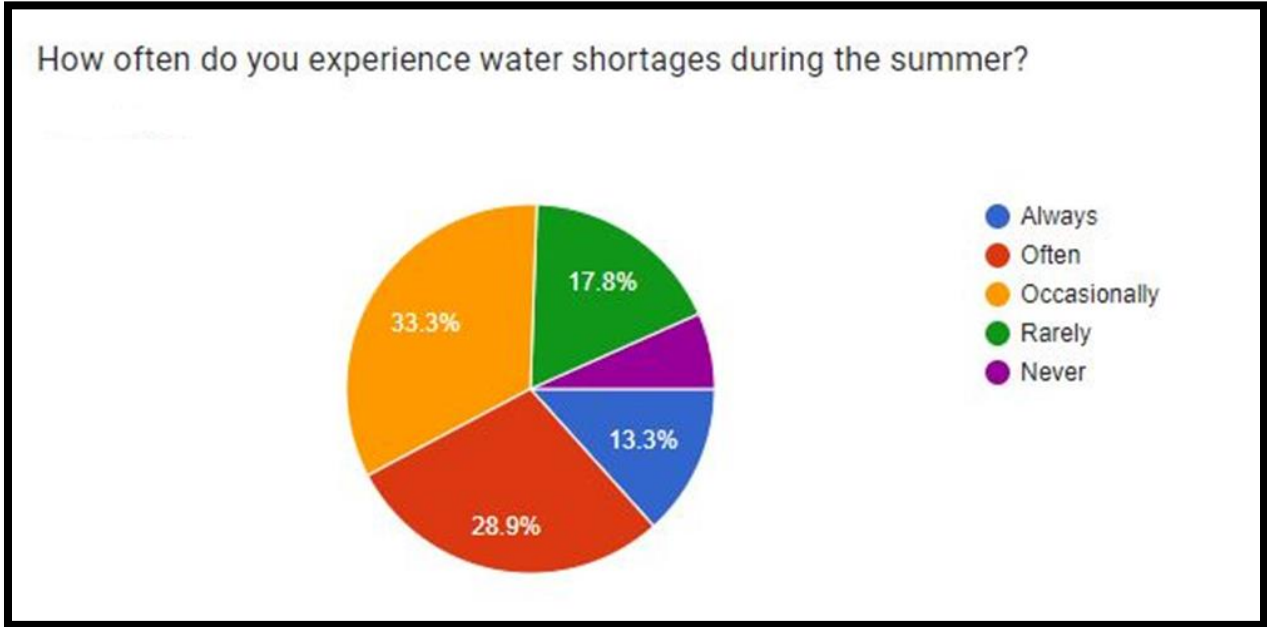


Figure 22. Survey question 5 response

Major findings:

- About 53% of the respondents believe that the severity of heat during the summer months is very high in their area.
- Heat exhaustion, dehydration and headaches are the major heat-related health impacts being experienced by respondents.
- About 53% of respondents experience more than 50% surge in their electricity bills during peak summer months.
- About 71% of respondents experience frequent power outages during the summers.
- About 29% of respondents often experience water shortages during the summers in the study region.

4.6. Relevance with Sustainable Development Goals

The study aligns with the goal 11 of the 17 sustainable development goals SDGs adopted by all United Nations members with the aim to transform the world and end major problems such as climate change, poverty, world hunger, gender equality, health and wellbeing, and responsible consumption and production. Goal 11 of the SDGs particularly deals with sustainable cities and communities and making cities and human settlements inclusive, safe, resilient, and sustainable. Pakistan faces major challenges in making its cities and communities sustainable as a large proportion of urban population in major cities like Rawalpindi lives in slums with poor living conditions. Urban sprawl in Rawalpindi has led to slum formation, congestion, and environmental degradation. High UTFVI in the city's major built-up areas highlights the need for better infrastructure management and urban planning to reduce heat stress and ensure sustainable urbanization. There is a need for adequate urban planning to accommodate the expanding population and promote a healthy living environment for all citizens.

CONCLUSION AND RECOMMENDATIONS

The study was conducted to assess the impact of urbanization on land surface temperature and the consequent effects on the intensity of urban heat islands in Rawalpindi. The study's results suggest that the built-up area increased from 74.5 square kilometers in 2003 to 227.7 square kilometers in 2023 with an increase of 206% over a time span of 20 years. The findings from the temporal change in land surface temperature particularly relevant to the built-up area indicate that the mean LST in 2003 was 34 °C that has significantly increased to 39 °C in 2023. With the increase in built-up area, the UTFVI response has increased and has become more severe, as indicated in the UTFVI maps. The majority of built-up area has transitioned from low to stronger UTFVI zone as it falls in the UTFVI range of 0.05 to 0.22 which indicates a strong heat island effect. The results of the survey suggest that the rising land surface temperature and resultant urban heat island effect is causing drastic impacts on the socio-economic factors such as population health and resource and energy consumption.

The following recommendations are suggested for reducing the current and potential heat island effect in the study region.

- Encourage the installation of green roofs, cool roof coatings and vertical gardens on buildings as they can lower the roof surface temperature, decreasing the amount of heat transferred into a residential or commercial building particularly in densely built areas such as Saddar, Raja Bazaar and Satellite Town.
- Encourage the construction of energy-efficient buildings with proper insulation, natural ventilation, and reflective glass in the societies being currently developed.

- Plant trees along streets where possible and install shade structures over sidewalks and public spaces.
- Encourage rainwater harvesting to reduce surface runoff and utilize it to irrigate urban green spaces.
- Creating small pocket parks or green spaces in vacant lots and converting underused paved areas into green spaces.
- Increasing use of renewable energy resources and upgrading to energy-efficient HVAC systems.

REFERENCES

1. Abir, F. A., Ahmmed, S., Sarker, S. H., & Fahim, A. U. (2021). Thermal and ecological assessment based on land surface temperature and quantifying multivariate controlling factors in Bogura, Bangladesh. *Heliyon*, 7(9). <https://doi.org/10.1016/j.heliyon.2021.e08012>
2. Ahmad, N., Waqas, T., Shafique, M., & Ullah, I. (2022). The Land Surface Temperature Dynamics and Its Impact on Land Cover in District Peshawar, Khyber Pakhtunkhwa. *International Journal of Environment and Geoinformatics*, 9(3). <https://doi.org/10.30897/ijegeo.890206>
3. Ameen, R. F. M., & Mourshed, M. (2017). Urban environmental challenges in developing countries—A stakeholder perspective. *Habitat International*, 64. <https://doi.org/10.1016/j.habitatint.2017.04.002>
4. Anbazu, J., & Antwi, N. S. (2023). Nexus Between Heat and Air Pollution in Urban Areas and the Role of Resilience Planning in Mitigating These Threats. *Advances in Environmental and Engineering Research*, 04(04). <https://doi.org/10.21926/aer.2304047>
5. Arshad, A., Ashraf, M., Sundari, R. S., Qamar, H., Wajid, M., & Hasan, M. ul. (2020). Vulnerability assessment of urban expansion and modelling green spaces to build heat waves risk resiliency in Karachi. *International Journal of Disaster Risk Reduction*, 46. <https://doi.org/10.1016/j.ijdr.2019.101468>
6. Asad, A., Ullah, K., Butt, M. J., & Labban, A. bin H. (2023). Analysis of urban heat island effects in high altitude areas of Pakistan. *Remote Sensing Applications: Society and Environment*, 32. <https://doi.org/10.1016/j.rsase.2023.101071>
7. Basit, M., & Shakrullah, K. (2019) Monitoring and analysis of urban heat Island of Lahore city in Pakistan during winter season, *European Journal of Climate Change* <https://doi.org/10.34154/2019-ejcc-0101-24-31>
8. Bernet, B. A., Peskura, E. T., Meyer, S. T., Bauch, P. C., & Donaldson, M. B. (2019). The effects of hip-targeted physical therapy interventions on low back pain: A systematic review and meta-analysis. In *Musculoskeletal Science and Practice* (Vol. 39). <https://doi.org/10.1016/j.msksp.2018.11.016>

9. Bimenyimana, T., Bugenimana, E. D., Habineza, E., Bushesha, M. S., & Ali, M. (2022). Impact of Urbanization on Land use and Land Cover Changes in Growing Cities of Rwanda. *Journal of Korean Society of Environmental Engineers*, 44(8). <https://doi.org/10.4491/ksee.2022.44.8.258>
10. Faisal, A. Al, Kafy, A. A., Al Rakib, A., Akter, K. S., Jahir, D. M. A., Sikdar, M. S., Ashrafi, T. J., Mallik, S., & Rahman, M. M. (2021). Assessing and predicting land use/land cover, Land Surface Temperature and urban thermal field variance index using Landsat imagery for Dhaka Metropolitan area. *Environmental Challenges*, 4. <https://doi.org/10.1016/j.envc.2021.100192>
11. Farid, N., Moazzam, M. F. U., Ahmad, S. R., Coluzzi, R., & Lanfredi, M. (2022). Monitoring the Impact of Rapid Urbanization on Land Surface Temperature and Assessment of Surface Urban Heat Island Using Landsat in Megacity (Lahore) of Pakistan. *Frontiers in Remote Sensing*, 3. <https://doi.org/10.3389/frsen.2022.897397>
12. Gorelick, N., Hancher, M., Dixon, M., Ilyushchenko, S., Thau, D., & Moore, R. (2017). Google Earth Engine: Planetary-scale geospatial analysis for everyone. *Remote Sensing of Environment*, 202. <https://doi.org/10.1016/j.rse.2017.06.031>
13. Ha, L. T. T., Trung, N. Van, Lan, P. T., Ai, T. T. H., & Hien, L. P. (2021). Impacts of urban land cover change on Land Surface Temperature distribution in Ho Chi Minh city, vietnam. *Journal of the Korean Society of Surveying, Geodesy, Photogrammetry and Cartography*, 39(2). <https://doi.org/10.7848/ksgpc.2021.39.2.113>
14. IPCC. (2022). IPCC Report 2022. *International Panel on Climate Change*.
15. Jabeen, N., Farwa, U.-, & Jadoon, Z. I. (2017). Urbanization in Pakistan : A Governance Perspective. *Journal of the Research Society of Pakistan*, 54(1).
16. Jain, S., Sannigrahi, S., Sen, S., Bhatt, S., Chakraborti, S., & Rahmat, S. (2020). Urban heat island intensity and its mitigation strategies in the fast-growing urban area. *Journal of Urban Management*, 9(1). <https://doi.org/10.1016/j.jum.2019.09.004>
17. Jothimani, M., Gunalan, J., Duraisamy, R., & Abebe, A. (2021). Study the Relationship Between LULC, LST, NDVI, NDWI and NDBI in Greater Arba Minch Area, Rift Valley, Ethiopia. *Proceedings of the 3rd International Conference on*

- Integrated Intelligent Computing Communication & Security (ICIIC 2021)*, 4.
<https://doi.org/10.2991/ahis.k.210913.023>
18. Kafy, A. Al, Rahman, M. S., Faisal, A. Al, Hasan, M. M., & Islam, M. (2020). Modelling future land use land cover changes and their impacts on Land Surface Temperatures in Rajshahi, Bangladesh. *Remote Sensing Applications: Society and Environment*, 18. <https://doi.org/10.1016/j.rsase.2020.100314>
 19. Kusumawardani, K. P., & Hidayati, I. N. (2022). Analysis of urban heat island and urban ecological quality based on remote sensing imagery transformation in semarang city. *IOP Conference Series: Earth and Environmental Science*, 1089(1). <https://doi.org/10.1088/1755-1315/1089/1/012037>
 20. Mejbel Salih, M., Zakariya Jasim, O., I. Hassoon, K., & Jameel Abdalkadhum, A. (2018). Land Surface Temperature Retrieval from LANDSAT-8 Thermal Infrared Sensor Data and Validation with Infrared Thermometer Camera. *International Journal of Engineering & Technology*, 7(4.20). <https://doi.org/10.14419/ijet.v7i4.20.27402>
 21. Moazzam, M. F. U., Doh, Y. H., & Lee, B. G. (2022). Impact of urbanization on Land Surface Temperature and surface urban heat Island using optical remote sensing data: A case study of Jeju Island, Republic of Korea. *Building and Environment*, 222. <https://doi.org/10.1016/j.buildenv.2022.109368>
 22. Murayama, Y., Simwanda, M., & Ranagalage, M. (2021). Spatiotemporal analysis of urbanization using GIS and remote sensing in developing countries. *Sustainability (Switzerland)*, 13(7). <https://doi.org/10.3390/su13073681>
 23. Nath, B., Ni-Meister, W., & Choudhury, R. (2021). Impact of urbanization on land use and land cover change in Guwahati city, India and its implication on declining groundwater level. *Groundwater for Sustainable Development*, 12. <https://doi.org/10.1016/j.gsd.2020.100500>
 24. Nuisssl, H., & Siedentop, S. (2021). *Urbanisation and Land Use Change*. https://doi.org/10.1007/978-3-030-50841-8_5
 25. Sajjad, S. H., Shahzad, K., Iqbal, T., & Ashraf, N. (2020a). Impact of urban evolution on local temperature trends of Rawalpindi and Islamabad. *European*

- Journal of Climate Change*, 2(2). <https://doi.org/10.34154/2020-ejcc-0202-33-46/auraass>
26. Sajjad, S. H., Shahzad, K., Iqbal, T., & Ashraf, N. (2020b). Impact of urban evolution on local temperature trends of Rawalpindi and Islamabad. *European Journal of Climate Change*, 2(2). <https://doi.org/10.34154/2020-ejcc-0202-33-46/auraass>
 27. Sameh, S., Zarzoura, F., & El-Mewafi, M. (2022). Automated Mapping of Urban Heat Island to Predict Land Surface Temperature and Land Use/Cover Change Using Machine Learning Algorithms: Mansoura City. *International Journal of Geoinformatics*, 18(6). <https://doi.org/10.52939/ijg.v18i6.2461>
 28. Sandoval, S., Escobar-Flores, J. G., & Badar Munir, M. (2023). Urbanization and its impacts on Land Surface Temperature and sea surface temperature in a tourist region in Mexico from 1990 to 2020. *Remote Sensing Applications: Society and Environment*, 32. <https://doi.org/10.1016/j.rsase.2023.101046>
 29. Singh, N., Singh, S., & Mall, R. K. (2020). Urban ecology and human health: implications of urban heat island, air pollution and climate change nexus. In *Urban Ecology: Emerging Patterns and Social-Ecological Systems*. <https://doi.org/10.1016/B978-0-12-820730-7.00017-3>
 30. Slimani, N., & Raham, D. (2023). Urban Growth Analysis Using Remote Sensing and GIS Techniques to Support Decision-Making In Algeria—The Case Of The City Of Setif. *Journal of the Geographical Institute Jovan Cvijic SASA*, 73(1). <https://doi.org/10.2298/IJGI2301017S>
 31. ul Haq, F., Naeem, U. A., Gabriel, H. F., Khan, N. M., Ahmad, I., Ur Rehman, H., & Zafar, M. A. (2021). Impact of Urbanization on Groundwater Levels in Rawalpindi City, Pakistan. *Pure and Applied Geophysics*, 178(2). <https://doi.org/10.1007/s00024-021-02660-y>
 32. U.S. Geological Survey. (2021). Landsat collection 2. *U.S. Geological Survey Fact Sheet 2021–3002, 1.1*(April).
 33. Waleed, M., & Sajjad, M. (2022). Leveraging cloud-based computing and spatial modeling approaches for Land Surface Temperature disparities in response to land

- cover change: Evidence from Pakistan. *Remote Sensing Applications: Society and Environment*, 25. <https://doi.org/10.1016/j.rsase.2021.100665>
34. Waleed, M., Sajjad, M., Acheampong, A. O., & Alam, M. T. (2023). Towards Sustainable and Livable Cities: Leveraging Remote Sensing, Machine Learning, and Geo-Information Modelling to Explore and Predict Thermal Field Variance in Response to Urban Growth. *Sustainability (Switzerland)* , 15(2). <https://doi.org/10.3390/su15021416>
35. Waseem, A., & Athar, H. (2022). LST variability and population growth in district of Rawalpindi, Pakistan during 1993–2018: A regional climate model based bias correction approach for LST. *Egyptian Journal of Remote Sensing and Space Science*, 25(4). <https://doi.org/10.1016/j.ejrs.2022.10.002>
36. Yang, L., Qian, F., Song, D. X., & Zheng, K. J. (2016). Research on Urban Heat-Island Effect. *Procedia Engineering*, 169. <https://doi.org/10.1016/j.proeng.2016.10.002>